AMERICAN SOCIETY FOR MICROBIOLOGY | Applied and Environmental Microbiology®

BIOTECHNOLOGY

Mediator Engineering of *Saccharomyces cerevisiae* To Improve Multidimensional Stress Tolerance

Yanli Qi,[a,b] Nan Xu,[c] Zehong Li,[d] Jiaping Wang,[a,b] Xin Meng,[a,b] Cong Gao,[a,b] Jian Chen,[a,b] Wei Chen,[a,b] Xiulai Chen,[a,b] Liming Liu[a,b]

[a]State Key Laboratory of Food Science and Technology, Jiangnan University, Wuxi, China
[b]International Joint Laboratory on Food Safety, Jiangnan University, Wuxi, China
[c]College of Bioscience and Biotechnology, Yangzhou University, Yangzhou, China
[d]School of Biotechnology, Jiangnan University, Wuxi, China

ABSTRACT *Saccharomyces cerevisiae* is a well-performing workhorse in chemical production, which encounters complex environmental stresses during industrial processes. We constructed a multiple stress tolerance mutant, Med15$^{V76R/R84K}$, that was obtained by engineering the KIX domain of Mediator tail subunit Med15. Med15$^{V76R/R84K}$ interacted with transcription factor Hap5 to improve *ARV1* expression for sterol homeostasis for decreasing membrane fluidity and thereby enhancing acid tolerance. Med15$^{V76R/R84K}$ interacted with transcription factor Mga2 to improve *GIT1* expression for phospholipid biosynthesis for increasing membrane integrity and thereby improving oxidative tolerance. Med15$^{V76R/R84K}$ interacted with transcription factor Aft1 to improve *NFT1* expression for inorganic ion transport for reducing membrane permeability and thereby enhancing osmotic tolerance. Based on this Med15 mutation, Med15$^{V76R/R84K}$, the engineered *S. cerevisiae* strain, showed a 28.1% increase in pyruvate production in a 1.0-L bioreactor compared to that of *S. cerevisiae* with its native Med15. These results indicated that Mediator engineering provides a potential alternative for improving multidimensional stress tolerance in *S. cerevisiae*.

IMPORTANCE This study identified the role of the KIX domain of Mediator tail subunit Med15 in response to acetic acid, H_2O_2, and NaCl in *S. cerevisiae*. Engineered KIX domain by protein engineering, the mutant strain Med15$^{V76R/R84K}$, increased multidimensional stress tolerance and pyruvate production compared with that of *S. cerevisiae* with its native Med15. The Med15$^{V76R/R84K}$ could increase membrane related genes expression possibly by enhancing interaction with transcription factor to improve membrane physiological functions under stress conditions.

KEYWORDS mediator engineering, gene expression, membrane physiological functions, multidimensional stress tolerance

Microbial fermentation of renewable feedstock represents an efficient and realistic solution to produce the desirable chemicals. During the industrial bioprocess, an industrial strain may encounter complex environmental stresses, such as temperature (1), acid (2), oxidative (3), and osmotic stress (4), which can negatively impact cell growth and inhibit metabolite production. Thus, stress tolerance is a critical physiological parameter for industrial strains. For this, several strategies have been built for evolving and achieving a robust industrial strain, such as enhancing the membrane barrier function by constructing lipid and cell wall (5), scavenging toxics by engineering transport system (6), regulating the general or specific transcription factors or coactivators (7), and activating signal transduction cascades (8). However, the achievement of single or multigene modifications is limited due to the complexity and multigenic control of stress response.

Editor Nicole R. Buan, University of Nebraska—Lincoln

Address correspondence to Liming Liu, mingll@jiangnan.edu.cn.

The authors declare no conflict of interest.

Received 13 August 2021
Accepted 8 March 2022
Published 4 April 2022

To address this problem, engineering the general and specific transcription regulators has been developed to regulate the transcriptional regulatory network (2, 9).

The transcriptional regulatory network could be regulated through manipulating and engineering native, artificial, and exogenous regulators (10, 11). First, the native regulators mainly contain general transcription factors in eukaryotic cells (e.g., *Saccharomyces cerevisiae*) (7), global regulator cyclic AMP receptor protein (CRP) (12) and specific transcription factors (13). Engineering the native regulators provides a promising strategy to enhance cell growth under stress condition. For example, when transcription factor Haa1 was overexpressed in *S. cerevisiae*, the intracellular acetic acid was decreased by about 31.8%, resulting in a large increase in acetate tolerance (14). Second, the rational or semirational design of artificial transcription factors (ATFs), based on the understanding of structure and function of zinc finger proteins, is a viable strategy to enhance stress tolerance (15). For example, using zinc-finger-based ATF, the maximum optical density at 620 nm (OD_{620}) of *S. cerevisiae* was increased by about 60% compared to that of wild-type strain in the presence of 5 g/L acetic acid (16). Third, exogenous regulators, such as Rky17, Sut2, and IrrE, have been introduced and modified to enhance stress tolerance (17–20). For example, when the heterologous expression of IrrE from *Deinococcus radiodurans* in *Arthrobacter simplex*, cell viability was increased by ~7-fold compared to that of wild-type strain under 16% (vol/vol) ethanol or 20% (vol/vol) methanol (21).

Mediator complex is a multisubunit conserved protein complex that is involved in nearly all gene expression in eukaryotic cells, which organizes into four modules: head, middle, tail, and cyclin-dependent kinase 8 (CDK8) (22–24). The tail module serves to recruit Mediator to sequence-specific transcription factors to active gene expression required for the response to environmental stress (including oxidative, salt, acid, and drug) (2, 25, 26). The Mediator tail subunit Med15 was first as Gal11 in *S. cerevisiae* (27, 28), which contained four structured domains: a KIX domain and activator-binding domains (ABDs) 1, 2, and 3 (29). The transcription factor-targeted three-helix bundle KIX domain in Med15 subunit was structurally conserved between mammals and yeast (30, 31). Here, to increase the multidimensional stress tolerance of *S. cerevisiae*, the KIX domains of Mediator tail subunit Med15 was identified as essential regulator and engineered by protein engineering. The final mutation strain, $Med15^{V76R/R84K}$, could enhance interaction between Med15 and transcription factors to change membrane fluidity, integrity, and permeability, thus increasing cell tolerance to acid, oxidative, and osmotic stresses.

RESULTS

The Med15 KIX domain was required for cell stress tolerance. To investigate the effect of environmental stress on the growth of BY4742, the half-maximal inhibitory concentrations (IC_{50}s) for acetic acid, H_2O_2, and NaCl were calculated. We found that its IC_{50} values were 0.25% (vol/vol), 2.8 mM, and 0.9 M, respectively (Fig. 1a). Thus, we selected 0.3% (vol/vol) acetic acid, 4 mM H_2O_2, or 1.2 M NaCl for further study due to the fact that cell growth was substantially inhibited, but sufficient biomass concentrations were still obtained under these conditions. In order to identify genes that are differentially regulated and therefore could contribute to the stress tolerance, transcriptome sequencing (RNA-seq) was conducted in BY4742 to compare global gene expression under YNB (0.67% yeast nitrogen base without amino acids, 2% glucose, containing histidine [20 mg/L], leucine [60 mg/L], lysine [200 mg/L], and uracil [20 mg/L]) medium and 0.3% (vol/vol) acetic acid, 4 mM H_2O_2, or 1.2 M NaCl conditions. The restrictive thresholds [$|\log_2(\text{fold change})| \geq 1.9$; false discovery rate < 0.05] of differentially expressed genes were used for further analysis.

Gene expression was analyzed. While many genes were up- or downregulated under only one stress condition, a considerable number changed expression for multiple stress conditions, with 87 genes differentially expressed under all the stress conditions (Fig. 1b; see List S1 in the supplemental material). In addition, Gene Ontology (GO) term enrichment analysis revealed that these 87 genes were involved in membrane transport, lipid metabolism, DNA replication and repair, the cell cycle, amino acid transport and metabolism, the translation signal transduction pathway, and

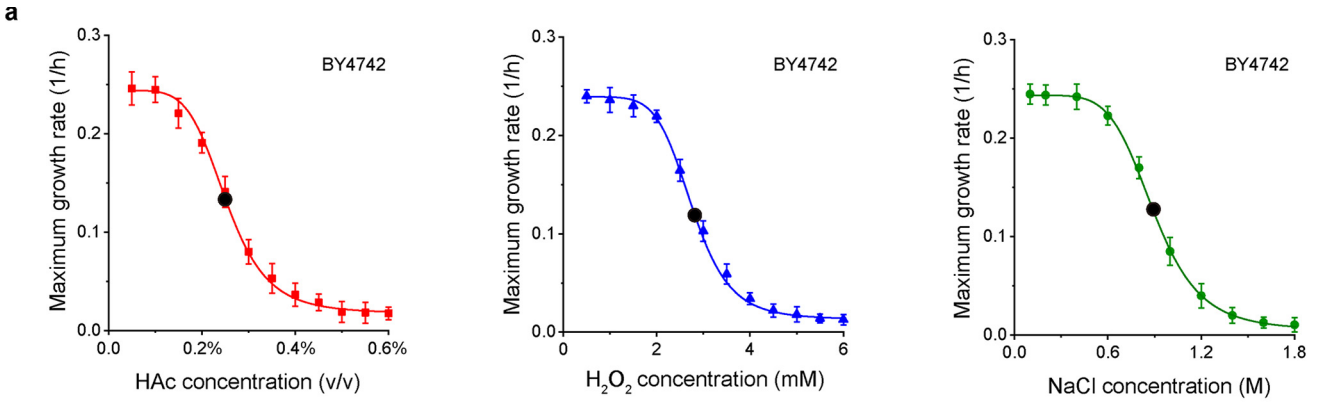

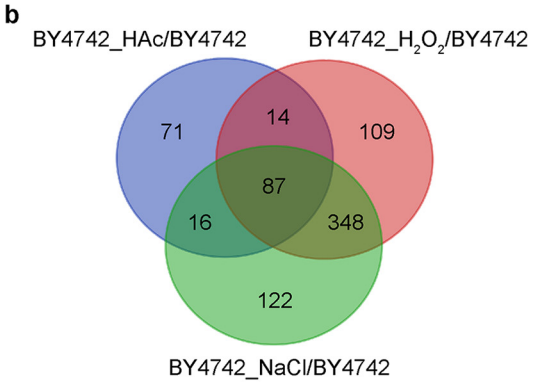

c

BY4742-HAc/BY4742		BY4742-H_2O_2/BY4742		BY4742-NaCl/BY4742	
Gene name	Fold change	Gene name	Fold change	Gene name	Fold change
INO1	4.1	*GIT1*	3.9	*LCB3*	4.7
ARV1	3.6	*ARV1*	3.9	*INO1*	3.4
PRY1	3.4	*INO1*	3.4	*GIT1*	2.9
QDR3	2.9	*ERG11*	3.0	*NFT1*	2.8
GIT1	2.9	*ELO3*	2.8	*ELO3*	2.8
MCD4	2.3	*PRY1*	2.5	*PRY1*	2.6
ELO3	2.0	*CHO2*	1.9	*MCD4*	2.4
CHO2	2.0	*MCD4*	1.9	*CHO2*	1.9

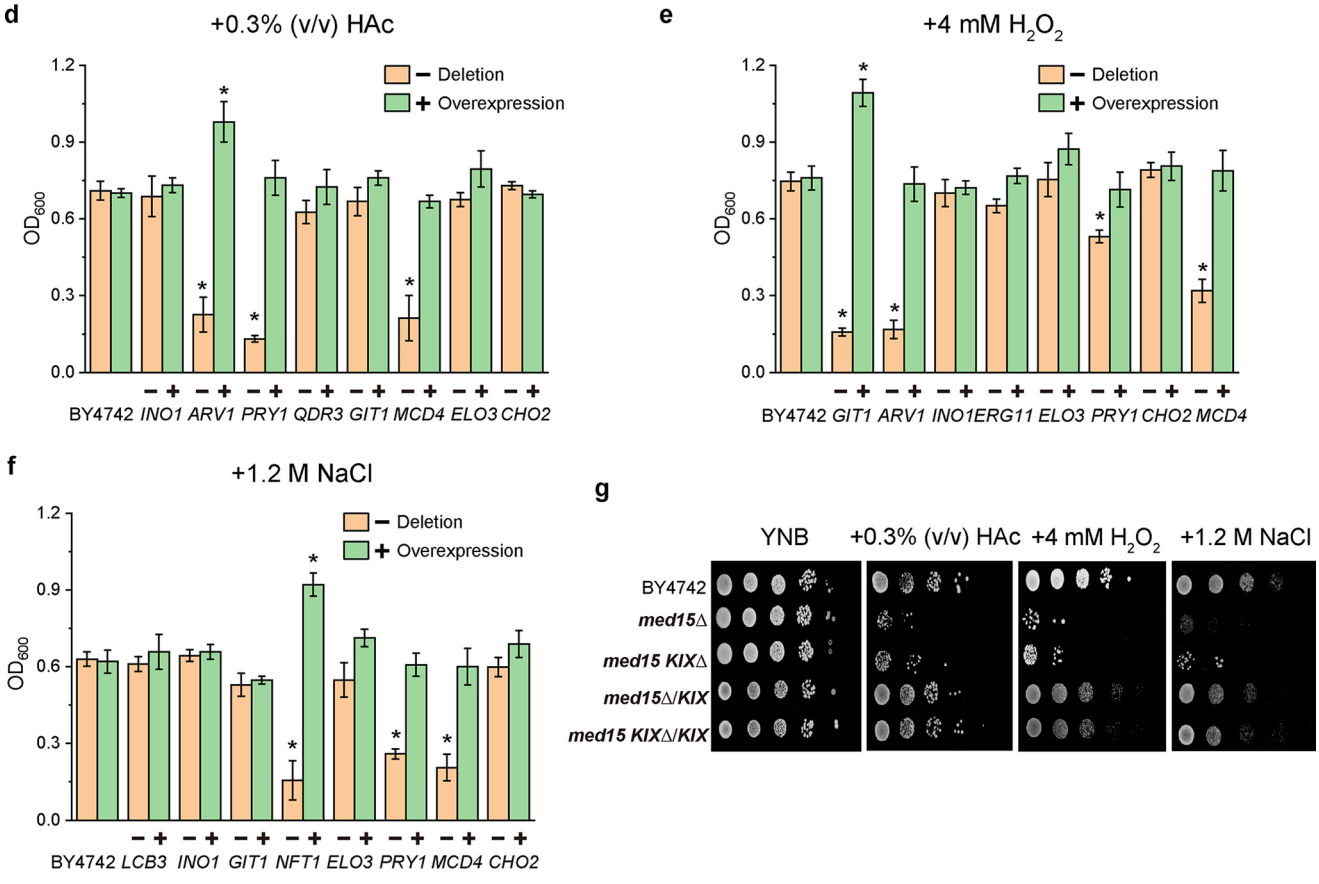

FIG 1 Med15 KIX domain was required for stress tolerance in *S. cerevisiae*. (a) Effect of acetic acid, H_2O_2, and NaCl on the IC_{50} of BY4742. (b) Gene expression overlap in BY4742 through transcription profile analysis under 0.3% (vol/vol) acetic acid, 4 mM H_2O_2, or 1.2 M NaCl conditions. (c) The most

(Continued on next page)

secondary metabolite biosynthesis (see Fig. S1). We concluded that membrane transport and lipid metabolism were the most notable differentially regulated pathways under all the stress conditions. Thus, membrane-related genes were proposed to respond to multidimensional stress conditions. The most significant differentially expressed genes involved in membrane transport and lipid metabolism (Fig. 1c; see also List S1 in the supplemental material)—especially for (i) eight genes under 0.3% (vol/vol) acetic acid, such as *INO1*, *ARV1*, *PRY1*, *QDR3*, *GIT1*, *MCD4*, *ELO3*, and *CHO2*, (ii) eight genes under 4 mM H_2O_2, such as *GIT1*, *ARV1*, *INO1*, *ERG11*, *ELO3*, *PRY1*, *CHO2*, and *MCD4*, and (iii) eight genes under 1.2 M NaCl, such as *LCB3*, *INO1*, *GIT1*, *NFT1*, *ELO3*, *PRY1*, *MCD4*, and *CHO2*—were selected, and the corresponding mutants were constructed and extensively characterized.

To test whether these genes were required for acid tolerance, we deleted or overexpressed *INO1*, *ARV1*, *PRY1*, *QDR3*, *GIT1*, *MCD4*, *ELO3*, and *CHO2* in BY4742. Compared to BY4742, the final biomasses of *arv1*Δ, *pry1*Δ, and *mcd4*Δ strains were decreased by 68.3, 81.5, and 70.1%, respectively, under 0.3% (vol/vol) acetic acid conditions, but the final biomass of *BY4742/ARV1* was increased by 37.8% (Fig. 1d). Then, to test whether these genes were required for oxidative tolerance, the genes *GIT1*, *ARV1*, *INO1*, *ERG11*, *ELO3*, *PRY1*, *CHO2*, and *MCD4* were deleted or overexpressed. Compared to that of BY4742, the final biomasses of *git1*Δ, *arv1*Δ, *pry1*Δ, and *mcd4*Δ strains were decreased by 78.9, 77.5, 29.8, and 57.3%, respectively, under 4 mM H_2O_2 condition, but the final biomass of *BY4742/GIT1* was increased by 43.7% (Fig. 1e). Finally, to test whether these genes were required for osmotic tolerance, the genes *LCB3*, *INO1*, *GIT1*, *NFT1*, *ELO3*, *PRY1*, *MCD4*, and *CHO2* were deleted or overexpressed. Compared to BY4742, the deletion of *NFT1*, *PRY1*, and *MCD4* led to 75.2, 58.9, and 67.3% decreases, respectively, in the final biomass under 1.2 M NaCl condition, but overexpression of *NFT1* showed a 48.5% increase (Fig. 1f). These results strongly demonstrated that *ARV1*, *GIT1*, and *NFT1* played important role in response to acid, oxidative, and osmotic stress, respectively.

In our previous studies, we found Mediator complex play an important role in the expression of genes in response to environmental stress (2, 32). To further explore the key Mediator complex subunit that can regulate acid, oxidative, and osmotic stress simultaneously, we examined the effect of 13 Mediator subunits on the tolerance of *S. cerevisiae* to acetic acid, H_2O_2, and NaCl stress. Among them, the subunit Med15, located at the tail module, was found to be essential for yeast stress tolerance (Fig. 2). Med15 consists of one KIX domain, three activator-binding domains (ABD1/2/3), and Q-rich linkers between the domains (29). The Med15 KIX domain can interact with various transcription factors to regulate several processes, such as stress response and multidrug resistance (30, 33). Thus, we further investigated whether the KIX domain deletion caused a similar phenotype with Med15 deletion. We found that deletion of the KIX domain decreased cell tolerance to acetic acid, H_2O_2, and NaCl, which was similar to the phenotype of the *med15*Δ strain (Fig. 1g). Importantly, cell growth was restored under acetic acid, H_2O_2, and osmotic stress by complementing *med15*Δ and *KIX*Δ strains with the KIX domain (Fig. 1g). Finally, we tested the expression level of *ARV1*, *GIT1*, and *NFT1* in *med15*Δ and *KIX*Δ strains and found that these genes were strongly downregulated under acetic acid, H_2O_2, and NaCl conditions, while the expression level of these genes was restored when complementing *med15*Δ and *KIX*Δ with the KIX domain (see Fig. S2). These results demonstrated that the Med15 KIX domain could help *S. cerevisiae* to resist acetic acid, H_2O_2, and NaCl stress.

Engineering the Med15 KIX domain to enhance cell stress tolerance. The activation domain (AD) of transcription factors could target the large hydrophobic groove harbored by the three helices of the Med15 KIX domain in yeast (Fig. 3a) (26, 31, 34), sug-

FIG 1 Legend (Continued)
differentially expressed genes were involved in membrane transport and lipid metabolism under acetic acid, H_2O_2, and osmotic stress. (d to f) Effect of gene deletion and overexpression on cell growth (OD_{600}) under 0.3% (vol/vol) acetic acid, 4 mM H_2O_2, or 1.2 M NaCl conditions, respectively. (g) Spot assays of BY4742, *med15*Δ, *med15KIX*Δ, *med15*Δ/KIX, and *med15KIX*Δ/KIX strains under 0.3% (vol/vol) acetic acid, 4 mM H_2O_2, or 1.2 M NaCl conditions, respectively. The experiments were performed in biological triplicates. Error bars indicate the standard deviations (*, $P < 0.05$ compared to that of the wild-type strain, as determined by a Student *t* test).

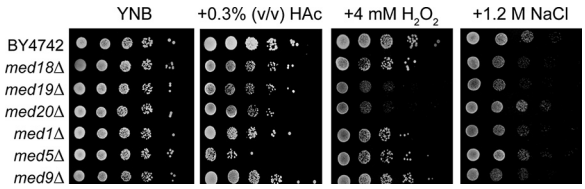

FIG 2 Med15 was required for *S. cerevisiae* tolerance to acetic acid, H_2O_2, and osmotic stress. Spot assays of *S. cerevisiae* with mediator subunit deletion under 0.3% (vol/vol) acetic acid, 4 mM H_2O_2, or 1.2 M NaCl conditions were performed.

gesting that the AD-KIX interaction interface might serve as a promising target for transcription factor ADs. Thus, we analyzed the interaction interfaces of the Med15 KIX domain with ADs of four transcription factors (Crz1, Hal9, Msn2, and Asg1 [13, 35, 36]) by Z-Dock analysis (26). These four transcription factors ADs targeted the same hydrophobic groove of the Med15 KIX domain, and the residues of the Med15 KIX domain interacted with four transcription factors ADs overlap strongly (Fig. 3b; see also Fig. S3).

Based on this, to test the effect of these overlap residues between Med15 and

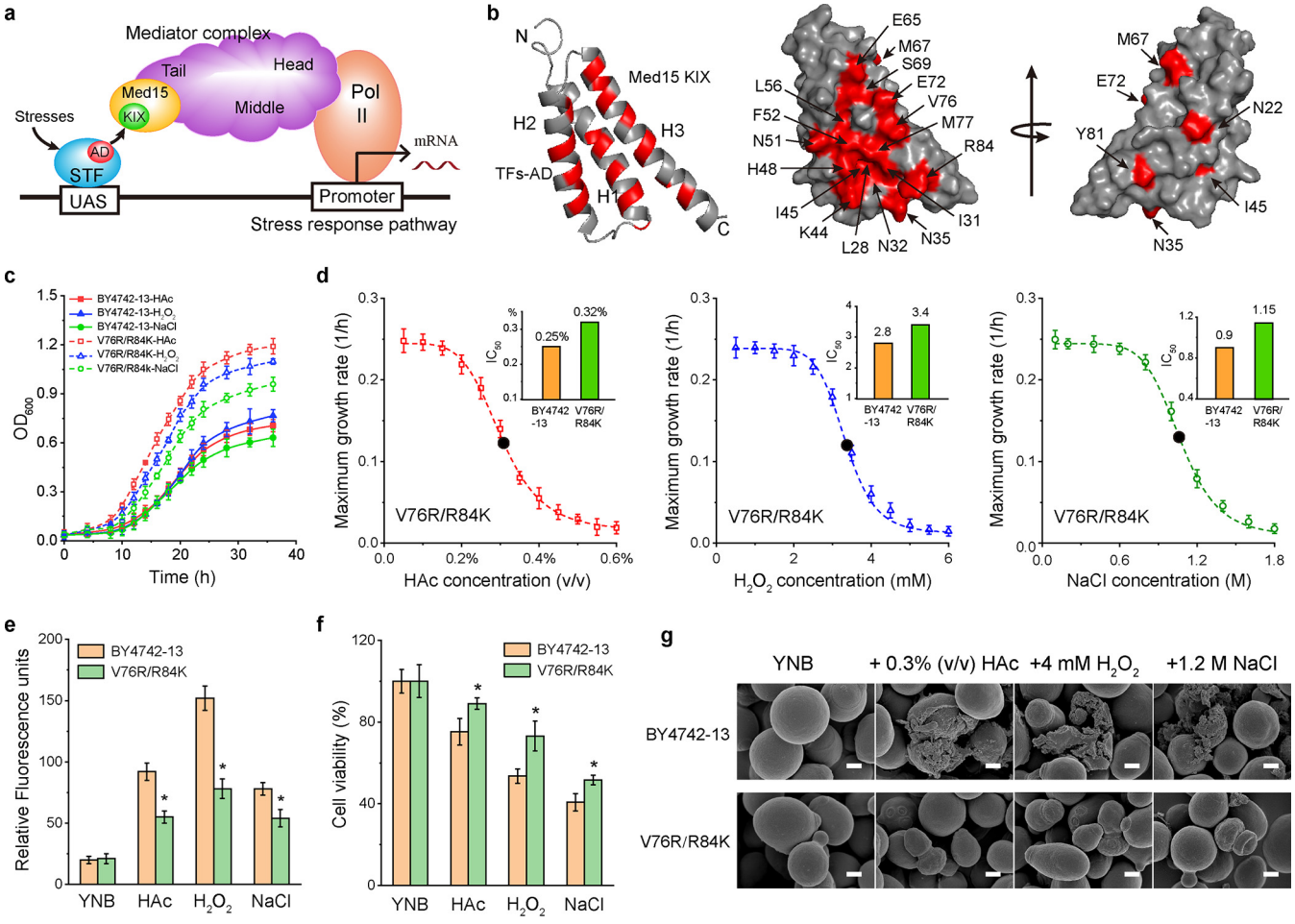

FIG 3 Engineering Med15 KIX domain to enhance stress tolerance in *S. cerevisiae*. (a) Mediator complex builds a bridge between specific transcription factors (STFs) and RNA polymerase II (Pol II). UAS, upstream active sequence; AD, activation domain. (b) Z-DOCK analysis showed that transcription factors ADs could bind to the same hydrophobic groove of the Med15 KIX domain. The overlap residues of the Med15 KIX domain (in red) interacted with four transcription factors ADs. (c) Effect of $Med15^{V76R/R84K}$ on cell growth (OD_{600}) under 0.3% (vol/vol) acetic acid, 4 mM H_2O_2, or 1.2 M NaCl conditions. (d) Effect of $Med15^{V76R/R84K}$ on the IC_{50} of *S. cerevisiae* under 0.3% (vol/vol) acetic acid, 4 mM H_2O_2, or 1.2 M NaCl conditions. (e) Effect of $Med15^{V76R/R84K}$ on the intracellular ROS level under 0.3% (vol/vol) acetic acid, 4 mM H_2O_2, or 1.2 M NaCl conditions. (f) Effect of $Med15^{V76R/R84K}$ on cell viability under 0.3% (vol/vol) acetic acid, 4 mM H_2O_2, or 1.2 M NaCl conditions. (g) Effect of $Med15^{V76R/R84K}$ on cell morphology under 0.3% (vol/vol) acetic acid, 4 mM H_2O_2, or 1.2 M NaCl conditions. Scale bars, 1 μm. The experiments were performed in biological triplicates. Error bars indicate the standard deviations (*, $P < 0.05$ compared to that of the wild-type strain, as determined by a Student *t* test).

transcription factors on KIX-dependent transcriptional responses and stress tolerance, six residues (N22, L24, L28, I31, N32, and N35) in helix 1, six residues (K44, I45, H48, N51, F52, and L56) in helix 2, and eight residues (E65, M67, S69, E72, V76, M77, Y81, and R84) in helix 3 from the interaction interface were chosen and then substituted by alanine. Among these mutations, the final biomasses of the mutant strains Med15^{I31A}, Med15^{H48A}, Med15^{N51A}, Med15^{E72A}, Med15^{V76A}, Med15^{Y81A}, and Med15^{R84A} were all higher than that of BY4742-13 (BY4742 with plasmid pY13) under acetic acid, H_2O_2, and NaCl stress (see Fig. S4). Thus, residues I31, H48, N51, E72, V76, Y81, and R84 were selected for further saturation mutagenesis, resulting in 672 candidate mutants. Among these mutations, the final biomasses of mutant strains Med15^{V76R} and Med15^{R84K} were all better than those of Med15^{V76A} and Med15^{R84A} under acetic acid, H_2O_2, and NaCl stress (see Fig. S4 and Table S2). Under the 0.3% (vol/vol) acetic acid condition, the final biomasses of mutant strains Med15^{V76R} and Med15^{R84K} were 0.99 and 1.03, which was increased by 11.2 and 9.6% compared those of Med15^{V76A} (0.89) and Med15^{R84A} (0.94), respectively. Under the 4 mM H_2O_2 condition, the final biomasses of mutant strains Med15^{V76R} and Med15^{R84K} were 1.04 and 1.02, which was increased by 5.8 and 7.5% compared to those of Med15^{V76A} (0.98) and Med15^{R84A} (0.95), respectively. Under the 1.2 M NaCl condition, the final biomasses of mutant strains Med15^{V76R} and Med15^{R84K} were 0.89 and 0.83, which was increased by 8.5 and 6.4% compared those of Med15^{V76A} (0.82) and Med15^{R84A} (0.78), respectively. Moreover, we investigated whether the double mutants further improve stress tolerance. Mutant strain Med15$^{V76R/R84K}$ was constructed and extensively characterized under stress conditions. Under the 0.3% (vol/vol) acetic acid condition, the final biomass of double mutant strain Med15$^{V76R/R84K}$ was 1.19, which was increased by 20.2, 15.5, and 67.6% compared to the biomasses of the Med15^{V76R}, Med15^{R84K}, and BY4742-13, respectively. Under the 4 mM H_2O_2 condition, the final biomass of double mutant strain Med15$^{V76R/R84K}$ was 1.10, which was increased by 5.8, 7.8, and 44.7% compared to the biomasses of Med15^{V76R}, Med15^{R84K}, and BY4742-13, respectively. Under the 1.2 M NaCl condition, the final biomass of double mutant strain Med15$^{V76R/R84K}$ was 0.96, which was increased by 7.9, 15.7, and 52.4% compared to the biomasses of Med15^{V76R}, Med15^{R84K}, and BY4742-13, respectively (Fig. 3c).

Finally, mutant strain Med15$^{V76R/R84K}$ led to 28.0, 21.4, and 27.8% increases in the IC_{50} for acetic acid, H_2O_2, and NaCl, respectively, compared to those of BY4742-13 (Fig. 3d). The intracellular reactive oxygen species (ROS) level was affected by all the stress conditions, and we found that the ROS levels in mutant strain Med15$^{V76R/R84K}$ were decreased by 40.2, 48.7, and 30.8%, respectively, compared to those of BY4742-13 under acetic acid, H_2O_2, and NaCl (Fig. 3e). Moreover, the cell viabilities of mutant strain Med15$^{V76R/R84K}$ were increased by 18.4, 36.7, and 22.5% under acetic acid, H_2O_2, and NaCl conditions (Fig. 3f), which was also confirmed by field emission scanning electron microscopy (FE-SEM) (Fig. 3g). Notably, BY4742-13 and mutant strain Med15$^{V76R/R84K}$ showed similarly healthy membrane morphology in YNB medium without stress conditions. BY4742-13 showed rough and broken membrane morphology under acetic acid, H_2O_2, and NaCl conditions, whereas mutant strain Med15$^{V76R/R84K}$ barely displayed any sign of membrane damage. These results demonstrated that Med15$^{V76R/R84K}$ could enhance yeast tolerance to acid, oxidative, and osmotic stress simultaneously.

Med15$^{V76R/R84K}$ enhanced acid tolerance by decreasing membrane fluidity. To investigate the effect of Med15$^{V76R/R84K}$ on *ARV1* expression on acid tolerance, the expression level of *ARV1* was determined. The expression level of *ARV1* was increased by 4.3-fold in mutant strain Med15$^{V76R/R84K}$ compared to that of BY4742-13 under the 0.3% (vol/vol) acetic acid condition (Fig. 4a). To further confirm this result, *ARV1* promoter was fused with enhanced green fluorescent protein (eGFP; P_{ARV1}-eGFP) and then introduced into *med15*Δ-13 and mutant strain Med15$^{V76R/R84K}$. eGFP fluorescence in *med15*Δ-13 could not be observed by fluorescence microscopy but could be observed in mutant strain Med15$^{V76R/R84K}$ (Fig. 4b). In addition, when P_{ARV1}-eGFP was introduced into BY4742-13 and mutant strain Med15$^{V76R/R84K}$, eGFP fluorescence was increased by 79.5% in mutant strain Med15$^{V76R/R84K}$ compared to that of BY4742-13 under the 0.3%

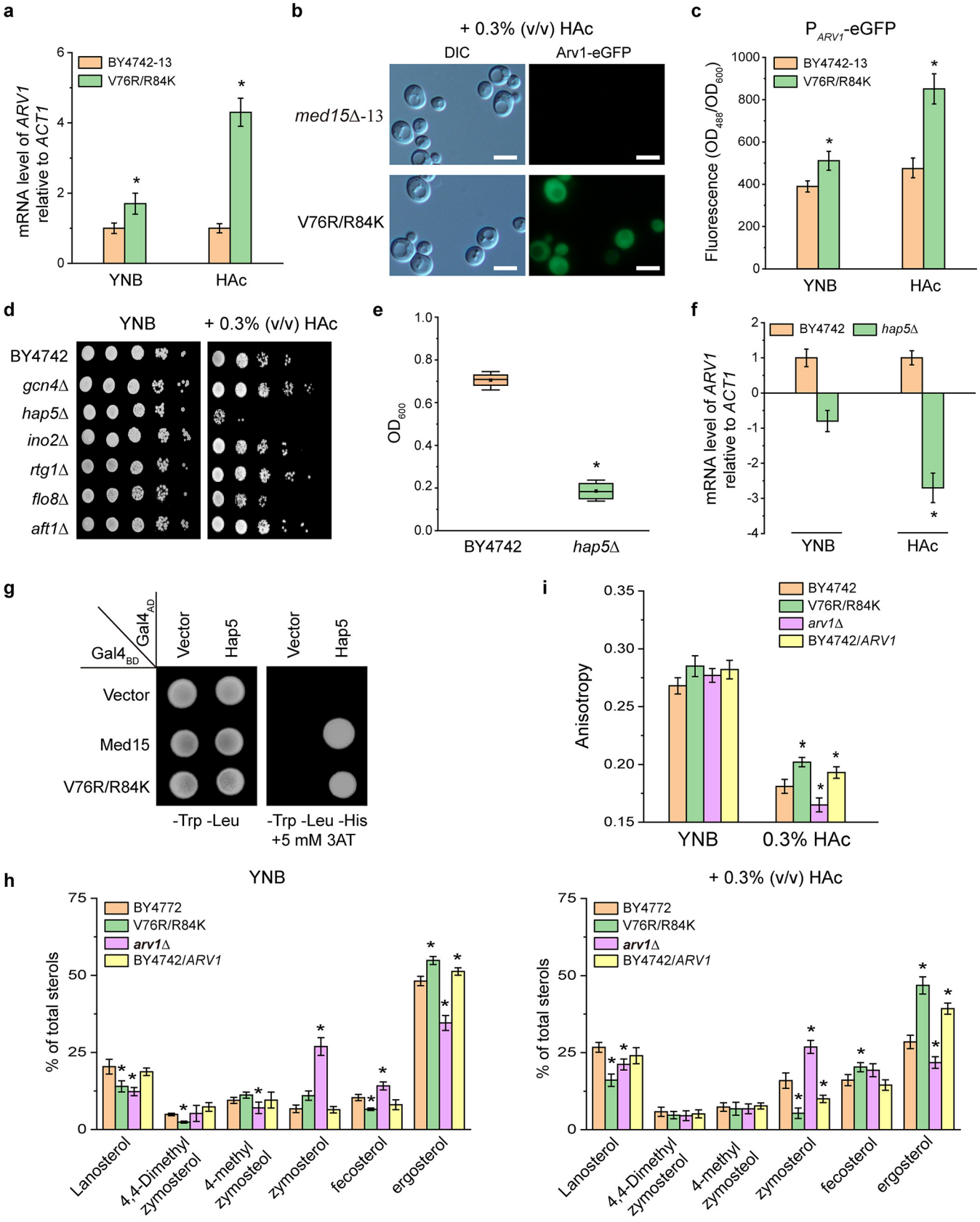

FIG 4 Med15$^{V76R/R84K}$ enhanced acid tolerance by decreasing membrane fluidity. (a) Effect of Med15$^{V76R/R84K}$ on the mRNA level of *ARV1* expression in *S. cerevisiae* under the 0.3% (vol/vol) acetic acid condition. (b) Effect of Med15$^{V76R/R84K}$ on *ARV1* promoter to drive the expression of eGFP reporter (P_{ARV1}-eGFP)

(Continued on next page)

(vol/vol) acetic acid condition (Fig. 4c). These results indicated that mutant strain Med15$^{V76R/R84K}$ could improve *ARV1* expression under acetic acid stress.

To investigate transcription factors involved in Med15$^{V76R/R84K}$-dependent *ARV1* expression under acetic acid stress, six transcription factors (Gcn4, Hap5, Ino2, Rtg1, Flo8, and Aft1) were selected according to transcriptome analysis (see Table S1 in the supplemental material). When they were respectively deleted, the *hap5*Δ strain showed a significant decrease in growth performance compared to those of other mutants under the 0.3% (vol/vol) acetic acid condition (Fig. 4d). In addition, *ARV1* expression and cell growth in *hap5*Δ were decreased by 2.7-fold and 72.9% compared to those of BY4742 (Fig. 4e and f). Further, a yeast two-hybrid (Y2H) analysis was carried out to determine whether Med15 (or Med15$^{V76R/R84K}$) interacted with Hap5 in response to acid stress (Fig. 4g). Cells expressing Gal4$_{BD}$-Med15 (or Gal4$_{BD}$-Med15$^{V76R/R84K}$) and Gal4$_{AD}$-Hap5 could grow on the medium without histidine, which indicated that Gal4$_{BD}$-Med15 (or Gal4$_{BD}$-Med15$^{V76R/R84K}$) could interact with Gal4$_{AD}$-Hap5 to form the active Gal4. These results suggested that Med15$^{V76R/R84K}$ could interacted with Hap5 to activate *ARV1* expression under acid stress.

Arv1 plays an important role in sterol homeostasis, which is involved in sterol uptake, trafficking and distribution into membranes (37). To test the effect of Med15$^{V76R/R84K}$ mutation and altered *ARV1* expression on membrane sterol composition in response to acid stress, the sterol composition of BY4742-13, mutant strain Med15$^{V76R/R84K}$, *arv1*Δ, and BY4742/*ARV1* strains in YNB medium with or without 0.3% (vol/vol) acetic acid were determined. Under the 0.3% (vol/vol) acetic acid condition, the proportion of ergosterol of *arv1*Δ was decreased by 23.4% compared to that of BY4742-13, whereas the proportion of ergosterol of BY4742/*ARV1* and mutant strain Med15$^{V76R/R84K}$ were increased by 37.9 and 64.4%, respectively (Fig. 4h). Because sterol distribution contributes to the fluidity of lipid membrane (38), which was further determined by steady-state anisotropy of diphenylhexatriene (DPH). As a result, the membrane fluidity of the *arv1*Δ strain was increased by 16.6% compared to that of BY4742-13 under the 0.3% (vol/vol) acetic acid condition, whereas the membrane fluidity of BY4742/*ARV1* and mutant strain Med15$^{V76R/R84K}$ were decreased by 8.3 and 14.4%, respectively (Fig. 4i). It is possible that mutant strain Med15$^{V76R/R84K}$ could decrease membrane fluidity by enhancing interaction between Med15 and Hap5 to improve *ARV1* expression for sterol homeostasis, thus enhancing acid tolerance.

Med15$^{V76R/R84K}$ improved oxidative tolerance by increasing membrane integrity. To investigate the effect of Med15$^{V76R/R84K}$ on *GIT1* expression on oxidative tolerance, the expression level of *GIT1* was determined. *GIT1* expression was increased by 3.6-fold in mutant strain Med15$^{V76R/R84K}$ compared to that of BY4742-13 under 4 mM H_2O_2 (Fig. 5a). To further confirm this result, *GIT1* promoter was fused with eGFP (P$_{GIT1}$-eGFP) and then introduced into the *med15*Δ-13 strain and the mutant strain Med15$^{V76R/R84K}$. eGFP fluorescence in strain *med15*Δ-13 could not be observed by fluorescence microscopy but could be observed in mutant strain Med15$^{V76R/R84K}$ (Fig. 5b). In addition, when P$_{GIT1}$-eGFP was introduced into BY4742-13 and mutant strain Med15$^{V76R/R84K}$, eGFP fluorescence was increased by 58.1% in mutant strain Med15$^{V76R/R84K}$ compared to that of BY4742-13 under 4 mM H_2O_2 (Fig. 5c). These results suggested that mutant strain Med15$^{V76R/R84K}$ could increase *GIT1* expression under oxidative stress.

To investigate transcription factors involved in Med15$^{V76R/R84K}$-dependent *GIT1* expression under oxidative stress, six transcription factors (Flo8, Yap1, Mig1, Ste12,

FIG 4 Legend (Continued)
in *med15*Δ-13 and mutant strain Med15$^{V76R/R84K}$ under the 0.3% (vol/vol) acetic acid condition. Scale bars, 5 μm. (c) Effect of Med15$^{V76R/R84K}$ on the green fluorescent of P$_{ARV1}$-eGFP in BY4742-13 and mutant strain Med15$^{V76R/R84K}$ under the 0.3% (vol/vol) acetic acid condition. (d) Growth performance of *S. cerevisiae* with transcription factor (Gcn4, Hap5, Ino2, Rtg1, Flo8, and Aft1) deletion under the 0.3% (vol/vol) acetic acid condition. (e) Effect of Hap5 deletion on cell growth (OD$_{600}$) under the 0.3% (vol/vol) acetic acid condition. (f) Effect of Hap5 deletion on the mRNA level of *ARV1* expression in the *hap5*Δ strain under the 0.3% (vol/vol) acetic acid condition. (g) Yeast two-hybrid assays were used to confirm the interaction between Med15 (or Med15$^{V76R/R84K}$) and Hap5. (h) Effect of Med15$^{V76R/R84K}$ and Arv1 on sterol homeostasis under the 0.3% (vol/vol) acetic acid condition. (i) Effect of Med15$^{V76R/R84K}$ and Arv1 on membrane fluidity under the 0.3% (vol/vol) acetic acid condition. The experiments were performed in biological triplicates. Error bars indicate the standard deviations (*, $P < 0.05$ compared to that of the wild-type strain, as determined by a Student *t* test).

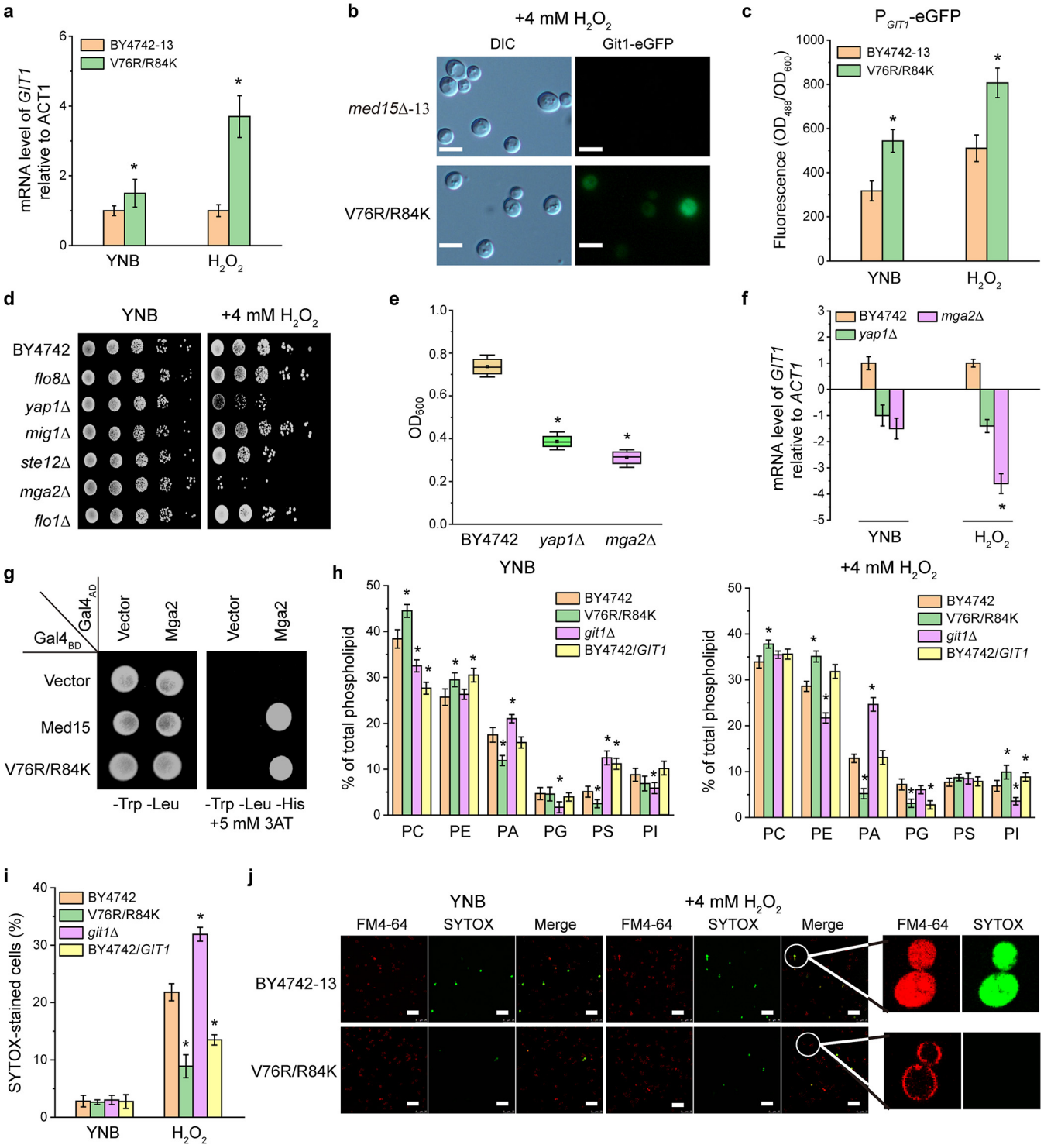

FIG 5 Med15$^{V76R/R84K}$ improved oxidative tolerance by increasing membrane integrity. (a) Effect of Med15$^{V76R/R84K}$ on the mRNA level of *GIT1* expression in *S. cerevisiae* under the 4 mM H_2O_2 condition. (b) Effect of Med15$^{V76R/R84K}$ on *GIT1* promoter to drive the expression of eGFP reporter (P_{GIT1}-eGFP) in *med15*Δ-13 and mutant strain Med15$^{V76R/R84K}$ under the 4 mM H_2O_2 condition. Scale bars, 5 μm. (c) Effect of Med15$^{V76R/R84K}$ on the green fluorescent of P_{GIT1}-eGFP in BY4742-13 and mutant strain Med15$^{V76R/R84K}$ under 4 mM H_2O_2 stress. (d) Growth performance of *S. cerevisiae* with transcription factor (Flo8, Yap1, Mig1, Ste12, Mga2, and Flo1) deletion under the 4 mM H_2O_2 condition. (e) Effect of Yap1 or Mga2 deletion on cell growth (OD_{600}) under the 4 mM H_2O_2 condition. (f) Effect of Yap1 or Mga2 deletion on the mRNA level of *GIT1* expression in *yap1*Δ and *mga2*Δ strains under the 4 mM H_2O_2 condition. (g) Yeast two-hybrid assays were used to confirm the interaction between Med15 (or Med15$^{V76R/R84K}$) and Mga2. (h) Effect of Med15$^{V76R/R84K}$ and *GIT1* on phospholipid biosynthesis under the 4 mM H_2O_2 condition. (i) Effect of Med15$^{V76R/R84K}$ and Git1 on membrane integrity analyzed by flow cytometry under the 4 mM H_2O_2 condition. (j) Effect of Med15$^{V76R/R84K}$ and Git1 on membrane integrity confirmed by LSCM under the 4 mM H_2O_2 condition. Scale bars, 15 μm. The experiments were performed in biological triplicates. Error bars indicate the standard deviations (*, $P < 0.05$ compared to that of the wild-type strain, as determined by a Student *t* test).

Mga2, and Flo1) were selected according to transcriptome analysis (see Table S1). When these genes were deleted respectively, the *yap1*Δ and *mga2*Δ mutant strains showed a significant decrease in growth performance compared to those of other mutants under 4 mM H_2O_2 (Fig. 5d). In addition, the final biomasses of *yap1*Δ and *mga2*Δ strains were decreased by 48.8 and 58.6%, respectively (Fig. 5e). Then, *GIT1* expression in *yap1*Δ and *mga2*Δ strains were reduced by 1.4- and 3.6-fold compared to those of BY4742 under 4 mM H_2O_2 condition (Fig. 5f), suggesting that Mga2 plays a major role in regulating *GIT1* expression. Further, a gene-specific interaction between Med15 (Med15$^{V76R/R84K}$) and Mga2 was observed under 4 mM H_2O_2 by Y2H assay (Fig. 5g). Cells expressing Gal4$_{BD}$-Med15 (or Gal4$_{BD}$-Med15$^{V76R/R84K}$) and Gal4$_{AD}$-Mga2 could grow on the medium without histidine, which indicated that Gal4$_{BD}$-Med15 (or Gal4$_{BD}$-Med15$^{V76R/R84K}$) could interact with Gal4$_{AD}$-Mga2 to form the active Gal4. These results suggested that Med15$^{V76R/R84K}$ could interacted with Mga2 to activate *GIT1* expression under oxidative stress.

Git1 has significant effect on phospholipid biosynthesis, which mediates uptake of both glycerophosphoinositol (GroPIns) and glycerophosphocholine (GroPCho) for further cellular metabolism (39). To test the effect of Med15$^{V76R/R84K}$ mutation and altered *GIT1* expression on the membrane phospholipid composition in response to oxidative stress, the phospholipid compositions of BY4742-13, mutant Med15$^{V76R/R84K}$, *git1*Δ, and BY4742/*GIT1* strains were measured in YNB medium with or without 4 mM H_2O_2. Under the 4 mM H_2O_2 condition, the proportion of phosphatidylinositol (PI) of the *git1*Δ strain was decreased by 48.1% compared to that of BY4742-13, whereas the proportions of PI of BY4742/*GIT1* and mutant strain Med15$^{V76R/R84K}$ were increased by 28.1 and 43.5%, respectively (Fig. 5h). Because phospholipid head distribution could affect membrane integrity (40), the membrane integrities of BY4742-13, mutant Med15$^{V76R/R84K}$, *git1*Δ, and BY4742/*GIT1* strains were further tested by SYTOX green staining with flow cytometry. As a result, the membrane integrity of *git1*Δ was decreased by 46.3% compared to that of BY4742-13 under the 4 mM H_2O_2 condition, whereas the membrane integrities of BY4742/*GIT1* and mutant strain Med15$^{V76R/R84K}$ were increased by 38.1 and 59.2%, respectively (Fig. 5i), and this result was also confirmed by laser scanning confocal microscopy (LSCM) (Fig. 5j). It is possible that Med15$^{V76R/R84K}$ could increase membrane integrity by enhancing interaction between Med15 and Mga2 to improve *GIT1* expression for regulating phospholipid biosynthesis, thus improving oxidative tolerance.

Med15$^{V76R/R84K}$ increased osmotic tolerance by reducing membrane permeability. To analyze the effect of Med15$^{V76R/R84K}$ on *NFT1* expression on osmotic tolerance, the expression level of *NFT1* was measured. *NFT1* expression was increased by 5.1-fold in mutant strain Med15$^{V76R/R84K}$ compared to that of BY4742-13 under 1.2 M NaCl condition (Fig. 6a). To further confirm this result, *NFT1* promoter was fused with eGFP (P_{NFT1}-eGFP), and then introduced into *med15*Δ-13 and mutant Med15$^{V76R/R84K}$ strains. eGFP fluorescence in *med15*Δ-13 could not be observed by fluorescence microscopy but could be observed in mutant strain Med15$^{V76R/R84K}$ (Fig. 6b). In addition, when P_{NFT1}-GFP was introduced into BY4742-13 and mutant strain Med15$^{V76R/R84K}$, eGFP fluorescence was increased by 86.2% in mutant strain Med15$^{V76R/R84K}$ compared to that of BY4742-13 under the 1.2 M NaCl condition (Fig. 6c). These results suggested that Med15$^{V76R/R84K}$ could increase *NFT1* expression under osmotic stress.

To investigate transcription factors involved in Med15$^{V76R/R84K}$-dependent *NFT1* expression, six transcription factors (Aft1, Cst6, Pdr3, Ste12, Hap5, and Flo8) were selected according to transcriptome analysis (see Table S1). When these genes were deleted respectively, the *aft1*Δ and *cst6*Δ strains showed significant decreases in growth performance compared to those of other mutants under the 1.2 M NaCl condition (Fig. 6d). In addition, the final biomasses of *aft1*Δ and *cst6*Δ strains were decreased by 63.9 and 47.2%, respectively (Fig. 6e). Then, *NFT1* expression levels in *aft1*Δ and *cst6*Δ strains were decreased by 3.8- and 1.4-fold compared to that of BY4742 under the 1.2 M NaCl condition (Fig. 6f), suggesting that Aft1 plays a major role in regulating *NFT1* expression. Further, a gene-specific interaction between Med15 (or Med15$^{V76R/}$

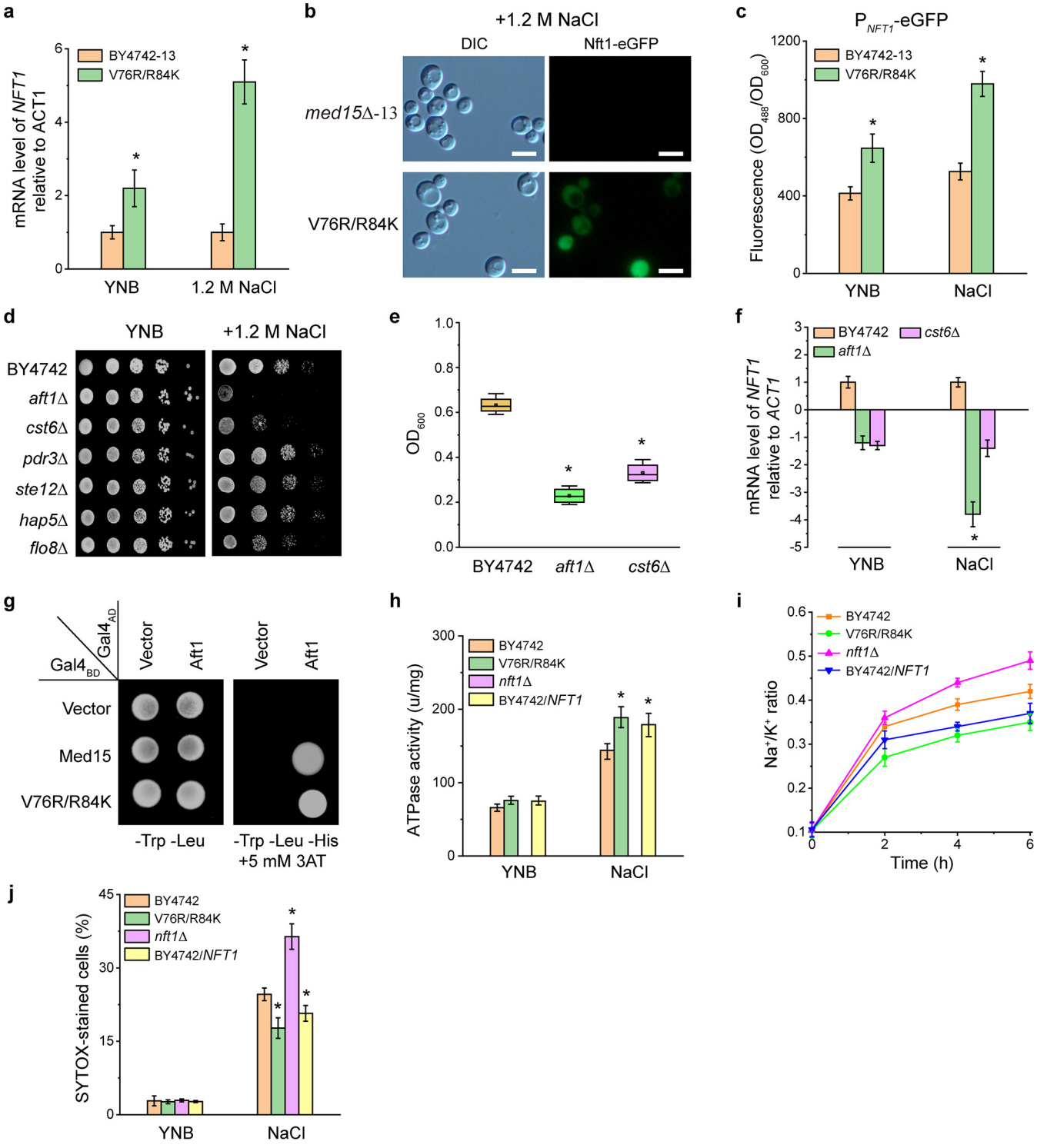

FIG 6 Med15$^{V76R/R84K}$ increased osmotic tolerance by reducing membrane permeability. (a) Effect of Med15$^{V76R/R84K}$ on the mRNA level of *NFT1* expression in *S. cerevisiae* under the 1.2 M NaCl condition. (b) Effect of Med15$^{V76R/R84K}$ on *NFT1* promoter to drive the expression of eGFP reporter (P_{NFT1}-eGFP) in *med15*Δ-13 and mutant strain Med15$^{V76R/R84K}$ under the 1.2 M NaCl condition. Scale bars, 5 μm. (c) Effect of Med15$^{V76R/R84K}$ on the green fluorescent of P_{NFT1}-eGFP in BY4742-13 and Med15$^{V76R/R84K}$ under the 1.2 M NaCl condition. (d) Growth performance of *S. cerevisiae* with transcription factor (Aft1, Cst6, Pdr3, Ste12, Hap5, and Flo8) deletion under the 1.2 M NaCl condition. (e) Effect of Aft1 or Cst6 deletion on cell growth (OD_{600}) under the 1.2 M NaCl condition. (f) Effect of Aft1 or Cst6 deletion on the mRNA level of *NFT1* expression in *aft1*Δ and *cst6*Δ strains under the 1.2 M NaCl condition. (g) Yeast two-hybrid assays were used to confirm the interaction between Med15 (or Med15$^{V76R/R84K}$) and Aft1. (h) Effect of Med15$^{V76R/R84K}$ on Nft1 activity under the 4 mM H_2O_2 condition. (i) Effect of Med15$^{V76R/R84K}$ and Nft1 on the ratio of intracellular Na^+ concentration to K^+ concentration under 4 mM H_2O_2 stress. (j) Effect of Med15$^{V76R/R84K}$ and Nft1 on membrane permeability under the 1.2 M NaCl condition. The experiments were performed in biological triplicates. Error bars indicate the standard deviations (*, $P < 0.05$ compared to that of the wild-type strain, as determined by a Student *t* test).

^{R84K}) and Nft1 was observed under 1.2 M NaCl by Y2H assay (Fig. 6g). Cells expressing $Gal4_{BD}$-Med15 (or $Gal4_{BD}$-Med15$^{V76R/R84K}$) and $Gal4_{AD}$-Aft1 could grow on the medium without histidine, which indicated that $Gal4_{BD}$-Med15 (or $Gal4_{BD}$-Med15$^{V76R/R84K}$) could interact with $Gal4_{AD}$-Aft1 to form the active Gal4. These results indicated that Med15$^{V76R/R84K}$ could interacted with Aft1 to activate *NFT1* expression under osmotic stress.

NFT1, encoding an ATP-binding cassette (ABC) transporter, plays an essential role in inorganic ion transport, which provides a translocation channel for inorganic ion to take part in further cellular metabolism (41). To test the effect of Med15$^{V76R/R84K}$ mutation and altered *NFT1* expression on the Nft1 activity and intracellular Na^+/K^+ ratio in response to osmotic stress, the Nft1 activities of BY4742-13, mutant Med15$^{V76R/R84K}$, *nft1*Δ, and BY4742/*NFT1* strains were measured in YNB medium with or without 1.2 M NaCl. Under the 1.2 M NaCl condition, the Nft1 activities of BY4742/*NFT1* and mutant strain Med15$^{V76R/R84K}$ were increased by 26.1 and 34.2% compared to that of BY4742-13, respectively, whereas the Nft1 activity could not be observed in the *nft1*Δ strain (Fig. 6h). As a result, after incubation in YNB medium with 1.2 M NaCl for 6 h, the intracellular Na^+/K^+ ratios of BY4742/*NFT1* and Med15$^{V76R/R84K}$ strains were decreased by 11.9 and 16.7% compared to that of BY4742-13, respectively, whereas the intracellular Na^+/K^+ ratio of the *nft1*Δ strain was increased by 16.7% (Fig. 6i). Because ABC transporters could affect membrane integrity, the membrane integrity were determined by SYTOX green staining with flow cytometry. The membrane integrity of BY4742/*NFT1* and mutant strain Med15$^{V76R/R84K}$ were increased by 28.5 and 47.6% compared to that of BY4742-13, respectively, whereas the membrane integrity of the *nft1*Δ strain was decreased by 15.9% under the 1.2 M NaCl condition (Fig. 6j). It is possible that Med15$^{V76R/R84K}$ could reduce membrane permeability by enhancing interaction between Med15 and Aft1 to improve *NFT1* expression for increasing inorganic ion transport, thus enhancing osmotic tolerance.

Med15$^{V76R/R84K}$ increased pyruvate production by enhancing stress tolerance. To investigate the applications of Mediator engineering in improving organic acid production, we tested whether Med15$^{V76R/R84K}$ could improve the performance of pyruvate production. The plasmid containing Med15$^{V76R/R84K}$ was introduced into pyruvate-producing strain *S. cerevisiae* TAM (TAM), obtained TAM Med15$^{V76R/R84K}$. Then, the pyruvate titers of TAM Med15$^{V76R/R84K}$ and TAM-13 (TAM with plasmid pY13) were determined without pH buffering. It was found that the final biomass and pyruvate titers of strain TAM Med15$^{V76R/R84K}$ were 6.8 and 31.2 g L^{-1} in a shaken flask, values which were increased by 25.9 and 17.7% compared to the corresponding values in TAM-13 (5.4 and 26.5 g L^{-1}) (see Fig. S5). To quantify the effect of Med15$^{V76R/R84K}$ on pyruvate production, the performances of TAM Med15$^{V76R/R84K}$ and TAM-13 were investigated in a 1.0-L bioreactor. The final biomass and highest pyruvate titer of TAM Med15$^{V76R/R84K}$ were achieved at 10.4 and 38.4 g L^{-1}, values which were increased by 26.8 and 28.1% compared to the corresponding values in TAM-13 (8.2 and 30.2 g L^{-1}) (Fig. 7a and b). In addition, the intracellular pH was determined, and we found that the intracellular pH of TAM Med15$^{V76R/R84K}$ was 6.5, which was higher than that of TAM-13 (5.8) (Fig. 7c). The intracellular ROS level was also determined, and we found that the ROS level in TAM Med15$^{V76R/R84K}$ was decreased by 24.7% compared to that of TAM-13 (Fig. 7d). Moreover, the cell morphology of TAM Med15$^{V76R/R84K}$ and TAM-13 were analyzed by FE-SEM, and we found that TAM Med15$^{V76R/R84K}$ could improve cell morphology (Fig. 7e). These results indicated that Med15$^{V76R/R84K}$ could increase pyruvate production by improving intracellular environment and cell morphology during fermentation process.

DISCUSSION

In this study, we found that Mediator tail subunit Med15 was required for stress tolerance, and its KIX domain was engineered to enhance the tolerance of environmental stress by protein engineering. The final Med15 mutation, Med15$^{V76R/R84K}$, could interact with transcription factors Hap5, Mga2 and Aft1 to increase the expression level of genes *ARV1*, *GIT1*, and *NFT1* under acid, oxidative, and osmotic conditions, respectively.

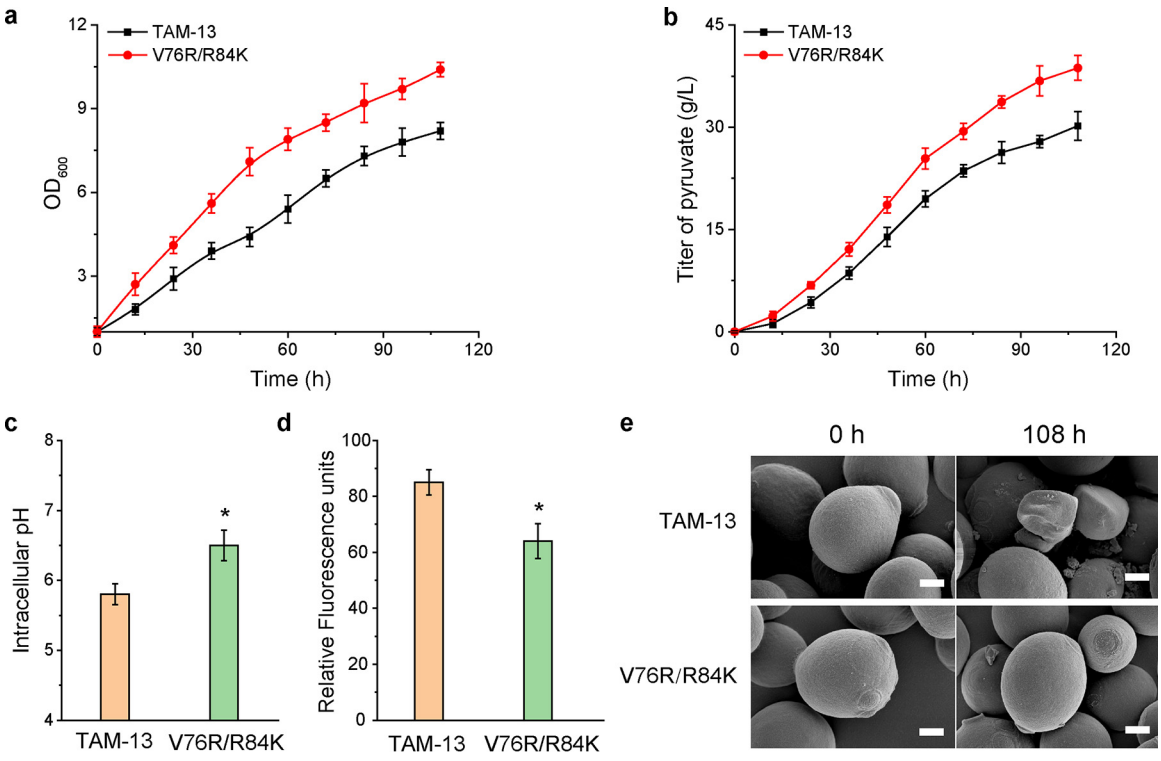

FIG 7 Med15$^{V76R/R84K}$ increased pyruvate production in bioreactor culture. (a) Effect of Med15$^{V76R/R84K}$ on cell growth (OD_{600}) during pyruvate production in a 1.0-L bioreactor. (b) Effect of Med15$^{V76R/R84K}$ on pyruvate titer in a 1.0-L bioreactor. (c) Effect of Med15$^{V76R/R84K}$ on the intracellular pH during pyruvate production in a 1.0-L bioreactor. (d) Effect of Med15$^{V76R/R84K}$ on the intracellular ROS level during pyruvate production in a 1.0-L bioreactor. (e) Effect of Med15$^{V76R/R84K}$ on cell morphology during pyruvate production in a 1.0-L bioreactor. Scale bars, 1 μm. The experiments were performed in biological triplicates. Error bars indicate the standard deviations (*, $P < 0.05$ compared to that of the wild-type strain, as determined by a Student *t* test).

As a result, the membrane fluidity, integrity, and permeability were changed to improve cell tolerance to acid, oxidative, and osmotic stress, leading to an increase in pyruvate production. These results open a new window for enhancing multidimensional stress tolerance to enhance chemical production by engineering mediator Med15 to improve membrane physiological function.

The Med15 KIX domain is successfully identified and engineered to enhance the tolerance of *S. cerevisiae* to complex environmental stress, such as acid, oxidative, and osmotic stress. Recently, a serial of strategies have been developed to enhance cell stress tolerance, including adaptive laboratory evolution, artificial mutagenesis, and stress response regulation (42–44). However, these strategies were not efficient for improving the tolerance of environmental stress due to the complexity process of stress response (42). Thus, researchers have to pay more attention to global transcription regulators such as H-NS (45), Spt15 (7), and cyclic AMP receptor protein (CRP) (46) and to specific transcription factors such as Cst6 (47) and Haa1 (48). Based on this idea, a series of methods have been developed to enhance the physiological functions of global transcription regulators, including gene deletion, gene overexpression, random mutagenesis, and DNA shuffling (9, 49, 50). For example, when Spt15^{K31Q} was expressed in *Kluyveromyces marxianus*, its ethanol tolerance was increased compared to that of wild-type strain in the presence of 6% (vol/vol) ethanol (7). Similarly, as an important global transcription regulator, the Med15 KIX domain could interact with the active domain (AD) of the transcription factor to change the expression level of Med15-dependent genes in the stress response process. For example, in *C. glabrata* (2, 25, 26), the Med15 KIX domain interacted with the Pdr1 AD to increase the expression level of efflux pump Pdr5, thus enhancing its multidrug resistance. In the present study, the Med15 KIX domain was rationally engineered to increase yeast tolerant to acetic acid,

H_2O_2, and osmotic stress. This strategy provides a potential method to increase the multidimensional stress tolerance of industrial strains.

Med15$^{V76R/R84K}$ could interact with the transcription factors Hap5, Mga2, and Aft1 to activate the membrane-related gene *ARV1*, *GIT1*, and *NFT1* expression in response to acid, oxidative, and osmotic stress, respectively. Here, we found that deletion or overexpression of most of significant differentially expressed genes did not affect the growth rate of the cell under the tested stress conditions. According to previous research, genetic stability could account for why this happens. Genetic stability can be mediated by multiple mechanisms: (i) genetic redundancy could replace inactivated genes to perform normal functions, or (ii) rewiring genetic network could deal with change/disturbance, or (iii) adaptive mutations to cope with lethal mutations and survive (51). In addition, the genetic compensation response (GCR) was recently proposed also as a possible explanation for the phenotypic discrepancies between gene knockout and gene knockdown (52, 53). Nonsense-mediated mRNA decay caused by gene deletion mutation could guide the transcription complex to activate homologous gene transcription (52). We found that *ARV1*, *GIT1*, and *NFT1* played important role in response to acid, oxidative, and osmotic stress, respectively. Two general ways have been developed to alter membrane functions through engineering global transcription factors to enhance the stress tolerance of an industrial strain. First, the Mediator complex directly regulates the expression level of membrane related genes to alter membrane functions (2, 32). For example, membrane integrity in *C. glabrata* was enhanced by overexpressing Med3 to upregulate the corresponding genes for fatty acid biosynthesis, leading to a 1.9-fold increase in cell viability at pH 2.0 (32). Second, the Mediator complex indirectly activates the membrane-related genes to alter membrane functions through transcription factors, such as Asg1, Rds2, and Crz1 (13, 35, 36). A good example is that Med15 is required for decanoic acid tolerance in *S. cerevisiae* by mediating interaction between Med15 and Oaf1 to activate gene expression, such as the genes *EEB1*, *FAA1*, and *ELO1*, in fatty acid metabolism (54). In the present study, Med15$^{V76R/R84K}$ was engineered and could enhance interaction between Med15 and Hap5, Mga2, and Aft1 to increase the expression levels of the genes *ARV1*, *GIT1*, and *NFT1* under acid, oxidative, and osmotic stress, respectively. These findings are not only important for enhancing multidimensional stress tolerance but also provide a better understanding of the mechanisms underlying the yeast response to multidimensional stress.

The robustness of industrial strains can be improved by changing membrane functions, such as membrane fluidity, integrity, and permeability. Membrane fluidity, integrity, and permeability can be affected by the type and content of sterols, the length and extent of unsaturation of membrane straight-chain fatty acids, the composition and distribution of phospholipids, and the activity of membrane proteins and the intracellular energy system (38, 55). Thus, a series of potential strategies, including metabolic, biochemical, and genetic engineering, were developed to change the functions and biophysical properties of microbial membranes through regulating their biosynthesis pathways and composition. First, membrane fluidity can be affected by the length and unsaturation of fatty acid chains and the composition of phospholipids and sterols (1, 56). For example, the membrane fluidity was changed by regulating desaturase (Ole1) to increase unsaturated fatty acids in *S. cerevisiae* (57) or expressing heterologous *cis-trans* isomerase (Cti) to introduce transunsaturated fatty acids in *Escherichia coli* (58), thus improving its cell tolerance to toxic products (such as octanoic acid and alcohols) and the adverse conditions (such as low pH and osmotic stress). In this study, the membrane fluidity in mutant strain Med15$^{V76R/R84K}$ was decreased to enhance stress tolerance to acetic acid, due to the increase of fecosterol and ergosterol content, which was consisted with the fact that a high ergosterol content could decrease membrane fluidity (59). Second, membrane integrity can be affected by membrane lipid composition (40, 43, 60, 61), membrane protein (such as fatty acid transporter OmpF and FadL) (62), and transcription regulators (such as Upc2, Ecm22, Rds2, Crz1, Med3, and Med15)

(2, 32, 35, 63, 64). For example, overexpression of *CDS1*, encoding phosphatidate cytidylyltransferase, and *CHO1*, encoding phosphatidylserine synthase in *S. cerevisiae*, showed found that its IC_{50} value for NaCl was increased by 17.8% compared to that of the wild-type strain (43). In the present study, the membrane integrity in mutant strain Med15$^{V76R/R84K}$ was increased to enhance oxidative tolerance due to the increase in PI proportion, which was consistent with the fact that phospholipid head distribution could be altered to increase membrane integrity (40). Third, membrane permeability is tightly related to membrane fluidity and integrity, which also can be regulated by engineering membrane lipids and proteins (such as transporters) (55). For example, membrane permeability in *S. cerevisiae* was reduced by deleting acetate transporter Ady2 to downregulate the intracellular pH and ROS level, thus enhancing acetic acid to improve acetic acid, ethanol, and H_2O_2 tolerance (65). In this study, the membrane permeability in mutant strain Med15$^{V76R/R84K}$ was improved to enhance stress tolerance to NaCl due to the increase in *NFT1* (ion transporter) expression. To sum up, mutant strain Med15$^{V76R/R84K}$ improved membrane fluidity, integrity, and permeability to enhance yeast tolerance to acid, oxidative, and osmotic stress simultaneously. These findings demonstrated that Mediator engineering provides an easy and convenient choice for improving membrane functions to enhance multidimensional stress tolerance simultaneously, an approach which may be widely used in industrial biotechnology.

An improvement in stress tolerance by Mediator engineering is crucial for increasing chemical production (40). In the past decade, some strategies have been developed to improve membrane physiological functions for enhancing stress tolerance of industrial strain, resulting in an increase of chemical production, such as transcription factor engineering, transporter engineering, metabolic engineering, and adaptive laboratory evolution (7, 40, 62). These strategies could enhance tolerance to some alcohol, short-chain fatty acid, and lipophilic compounds and increase their titers. For example, using metabolic engineering strategies to genetically modulate the proportion of phosphoethanolamine (PE) in *E. coli* was associated with a significant increase in membrane integrity, which not only enhanced tolerance to exogenous octanoic acid (C_8) but also remarkably increased the C_8 titer (40). However, due to the complexity of regulatory networks involved in stress response and chemical production, enhanced stress tolerance does not always lead to an increase in chemical production (63, 66). Here, membrane physiological functions were improved by rational engineered Med15 KIX domain, resulting in an increase in multidimensional stress tolerance and pyruvate production.

In conclusion, Mediator engineering provides a potential way to change membrane function and biophysical properties, thus increasing yeast tolerance to acid, oxidative, and osmotic stress. With the development of biotechnology, it is possible to efficiently and rationally manipulate multidimensional stress tolerance based on a better understanding of mechanisms for global transcription regulator-mediated stress tolerance. Furthermore, Mediator engineering may provide an easy and convenient approach for improving microbial cell factories for desirable chemical production in the future.

MATERIALS AND METHODS

Strains, plasmids, and growth conditions. The strains and plasmids used in this study are listed in Table 1 and Table 2, respectively. *E. coli* JM109 was used as the host to construct all plasmids. *S. cerevisiae BY4742* (*MATα his3*Δ1 *leu2*Δ0 *lys2*Δ0 *ura3*Δ0) was used as the wild-type strain to construct all the mutant strains. The deletion and replacement strains were constructed by CRISPR/Cas9 technology with plasmid pML104 (67). For the overexpression strains, the target genes were amplified from the genome of *BY4742* and cloned into pY26 driving with the GPD promoter. The recombinant plasmids were then transformed into *BY4742* generated the corresponding overexpression strains. Site-specific mutations were performed by a PCR-based method using the mutagenic primers. All of the primers used in this study are listed in Table 3.

Yeast cells were cultivated in YPD medium (1% yeast extract, 2% tryptone, and 2% glucose) and YNB medium (0.67% yeast nitrogen base without amino acids, 2% glucose, containing histidine [20 mg/L], leucine [60 mg/L], lysine [200 mg/L], and uracil [20 mg/L]). Yeast cells were incubated at 30°C with shaking at 200 rpm.

TABLE 1 Strains used in this study

Strain	Genotype	Source or reference
E. coli JM109		Our laboratory
S. cerevisiae		
BY4742	*MATα his3*Δ1*leu2*Δ0*lys2*Δ0*ura3*Δ0	Our laboratory
*med18*Δ	BY4742 *med18*Δ::*KanMX4*	73
*med19*Δ	BY4742 *med19*Δ::*KanMX4*	73
*med20*Δ	BY4742 *med20*Δ::*KanMX4*	73
*med1*Δ	BY4742 *med1*Δ::*KanMX4*	73
*med5*Δ	BY4742 *med5*Δ::*KanMX4*	73
*med9*Δ	BY4742 *med9*Δ::*KanMX4*	73
*med31*Δ	BY4742 *med31*Δ::*KanMX4*	73
*med2*Δ	BY4742 *med2*Δ::*KanMX4*	73
*med3*Δ	BY4742 *med3*Δ::*KanMX4*	73
*med15*Δ	BY4742 *med15*Δ::*KanMX4*	73
*med16*Δ	BY4742 *med16*Δ::*KanMX4*	73
*cdk8*Δ	BY4742 *cdk8*Δ::*KanMX4*	73
*cycc*Δ	BY4742 *cycc*Δ::*KanMX4*	73
*med15 KIX*Δ	BY4742 *med15 KIX*Δ::*KanMX4*	This study
*med15*Δ*/KIX*	BY4742 *med15*Δ::*HIS3* pY13-P_{MED15}/*MED15 KIX*	This study
*med15 KIX*Δ*/KIX*	BY4742 *med15 KIX*Δ::*HIS3* pY13-P_{MED15}/*MED15 KIX*	This study
BY4742-13	BY4742::*HIS3* pY13	This study
$Med15^{V76R/R84K}$	BY4742 *med15*Δ::*HIS3* pY13-P_{MED15}/$Med15^{V76R/R84K}$	This study
*ino1*Δ	BY4742 *ino1*Δ::*KanMX4*	This study
*arv1*Δ	BY4742 *arv1*Δ::*KanMX4*	This study
*pry1*Δ	BY4742 *pry1*Δ::*KanMX4*	This study
*elo3*Δ	BY4742 *elo3*Δ::*KanMX4*	This study
*qdr2*Δ	BY4742 *qdr2*Δ::*KanMX4*	This study
*cho2*Δ	BY4742 *cho2*Δ::*KanMX4*	This study
*git1*Δ	BY4742 *git1*Δ::*KanMX4*	This study
*mcd4*Δ	BY4742 *mcd4*Δ::*KanMX4*	This study
*erg11*Δ	BY4742 *erg11*Δ::*KanMX4*	This study
*plb1*Δ	BY4742 *plb1*Δ::*KanMX4*	This study
*lcb1*Δ	BY4742 *lcb1*Δ::*KanMX4*	This study
*nft1*Δ	BY4742 *nft1*Δ::*KanMX4*	This study
BY4742-26	BY4742::*URA3* pY26	This study
BY4742/*INO1*	BY4742::*URA3* pY26-P_{GPD}/*INO1*	This study
BY4742/*ARV1*	BY4742::*URA3* pY26-P_{GPD}/*ARV1*	This study
BY4742/*PRY1*	BY4742::*URA3* pY26-P_{GPD}/*PRY1*	This study
BY4742/*ELO3*	BY4742::*URA3* pY26-P_{GPD}/*ELO3*	This study
BY4742/*QDR2*	BY4742::*URA3* pY26-P_{GPD}/*QDR2*	This study
BY4742/*CHO2*	BY4742::*URA3* pY26-P_{GPD}/*CHO2*	This study
BY4742/*GIT1*	BY4742::*URA3* pY26-P_{GPD}/*GIT1*	This study
BY4742/*MCD4*	BY4742::*URA3* pY26-P_{GPD}/*MCD4*	This study
BY4742/*ERG11*	BY4742::*URA3* pY26-P_{GPD}/*ERG11*	This study
BY4742/*PLB1*	BY4742::*URA3* pY26-P_{GPD}/*PLB1*	This study
BY4742/*LCB1*	BY4742::*URA3* pY26-P_{GPD}/*LCB1*	This study
BY4742/*NFT1*	BY4742::*URA3* pY26-P_{GPD}/*NFT1*	This study
NFT1-HA	BY4742::*URA3* pY26-P_{GPD}/*NFT1-HA*	This study
$Med15^{V76R/R84K}$/*NFT1-HA*	BY4742 *med15*Δ::*HIS3* pY13-P_{MED15}/$Med15^{V76R/R84K}$/*NFT1-HA*	This study
BY4742-13/*NFT1-HA*	BY4742::*HIS3* pY13/*NFT1-HA*	This study
*med15*Δ 13	BY4742 *med15*Δ::*KanMX4*::*HIS3* pY13	This study
*med15*Δ-13/P_{ARV1}-*eGFP*	BY4742 *med15*Δ::*KanMX4*::*HIS3* pY13, ::*LEU2* YEplac181-P_{ARV1}/*eGFP*	This study
*med15*Δ-13/P_{GIT1}-*eGFP*	BY4742 *med15*Δ::*KanMX4*::*HIS3* pY13, ::*LEU2* YEplac181-P_{GIT1}/*eGFP*	This study
*med15*Δ-13/P_{NFT1}-*eGFP*	BY4742 *med15*Δ::*KanMX4*::*HIS3* pY13, ::*LEU2* YEplac181-P_{NFT1}/*eGFP*	This study
BY4742-13/P_{ARV1}-*eGFP*	BY4742::*HIS3* pY13, ::*LEU2* YEplac181-P_{ARV1}/*eGFP*	This study
BY4742-13/P_{GIT1}-*eGFP*	BY4742::*HIS3* pY13, ::*LEU2* YEplac181-P_{GIT1}/*eGFP*	This study
BY4742-13/P_{NFT1}-*eGFP*	BY4742::*HIS3* pY13, ::*LEU2* YEplac181-P_{NFT1}/*eGFP*	This study
$Med15^{V76R/R84K}$ /P_{ARV1}-*eGFP*	$Med15^{V76R/R84K}$::*LEU2* YEplac181-P_{ARV1}/*eGFP*	This study
$Med15^{V76R/R84K}$ /P_{GIT1}-*eGFP*	$Med15^{V76R/R84K}$::*LEU2* YEplac181-P_{GIT1}/*eGFP*	This study
$Med15^{V76R/R84K}$ /P_{NFT1}-*eGFP*	$Med15^{V76R/R84K}$::*LEU2* YEplac181-P_{NFT1}/*eGFP*	This study
*gcn4*Δ	BY4742 *gcn4*Δ::*KanMX4*	This study
*hap5*Δ	BY4742 *hap5*Δ::*KanMX4*	This study

(Continued on next page)

TABLE 1 (Continued)

Strain	Genotype	Source or reference
*ino2*Δ	BY4742 *ino2*Δ::*KanMX4*	This study
*rtg1*Δ	BY4742 *rtg1*Δ::*KanMX4*	This study
*flo8*Δ	BY4742 *flo8*Δ::*KanMX4*	This study
*yap1*Δ	BY4742 *yap1*Δ::*KanMX4*	This study
*mig1*Δ	BY4742 *mig1*Δ::*KanMX4*	This study
*ste12*Δ	BY4742 *ste12*Δ::*KanMX4*	This study
*mga2*Δ	BY4742 *mga2*Δ::*KanMX4*	This study
*flo1*Δ	BY4742 *flo1*Δ::*KanMX4*	This study
*aft1*Δ	BY4742 *aft1*Δ::*KanMX4*	This study
*cst6*Δ	BY4742 *cst6*Δ::*KanMX4*	This study
*pdr3*Δ	BY4742 *pdr3*Δ::*KanMX4*	This study
AH109	*trp1*Δ *leu2-ura3*Δ *his3*Δ *gal4*Δ *gal80*Δ *LYS2*::*GAL1*$_{UAS}$-*GAL1*$_{TATA}$-*HIS3* *GAL2*$_{UAS}$*GAL2*$_{TATA}$-*ADE2 URA3*::*MEL1*$_{UAS}$-*MEL1*$_{TATA}$-*LacZ MEL1*	Our laboratory
TAM-13	TAM::*HIS3* pY13	This study
TAM Med15$^{V76R/R84K}$	TAM *med15*Δ::*HIS3* pY13-P$_{MED15}$/Med15$^{V76R/R84K}$	This study

Spot assay, growth, and viability analysis. Log-phase cells were inoculated into liquid YNB medium supplemented with 0.05 to 0.60% (vol/vol) acetic acid, 0.5 to 6 mM H_2O_2, or 0.1 to 1.8 M NaCl with an initiation OD_{600} of 0.1. The OD_{600} values were recorded every 2 h until reaching stationary phase and used to draw a growth curve. The maximum specific growth rate was calculated for acetic acid (H_2O_2 or NaCl) concentration, yielding a half-maximal inhibitory concentration (IC_{50}). For the spot assay, cells were diluted in sterile water to an OD_{600} of 1.0. Serial dilutions (10-fold) of 4 μL were spotted on YNB plates with or without 0.3% (vol/vol) acetic acid (4 mM H_2O_2 or 1.2 M NaCl) and then incubated at 30°C for 3 to 5 days. For viability analysis, cells were cultured in YNB medium with or without 0.3% (vol/vol) acetic acid (4 mM H_2O_2 or 1.2 M NaCl) for 8 h, plated on YNB medium, and then incubated at 30°C for 3 to 5 days. The colonies were counted to analyze cell viability.

Measurement of intracellular reactive oxygen species. The intracellular ROS level was measured using the cell permeable probe (2′,7′-dichloro-dihydro-fluorescein diacetate [DCFH-DA]; Sigma-Aldrich) (68). In brief, after incubation in YNB medium with or without 0.3% (vol/vol) acetic acid (4 mM H_2O_2 or 1.2 M NaCl) for 2 h, the cells were collected, diluted in phosphate-buffered saline (PBS) to an OD_{600} of 1.0, and then treated with dithiothreitol and snailase to weaken the cell wall. Then, 10 μL of 1 mM DCFH-DA was added to 1-mL samples and subsequently mixed and incubated at 37°C for 40 min. The cells were washed three times to remove excess probe and then resuspended in PBS. The fluorescence intensity was measured at an excitation wavelength of 488 nm and an emission wavelength of 525 nm using flow cytometry (FACSAria; Becton Dickinson, USA).

Total RNA extraction and RNA-seq. Log-phase cells were incubated in YNB medium with or without 0.3% (vol/vol) acetic acid (4 mM H_2O_2 or 1.2 M NaCl) for 8 h. Total RNA was isolated using a MiniBEST universal RNA extraction kit (TaKaRa Bio, Shiga, Japan). The concentration and quality of total RNA were determined by microspectrophotometry using an Agilent 2100 Bioanalyzer (Agilent Technologies, Santa Clara, CA). Frozen samples were sent to the Majorbio Institute for global transcriptome analysis.

qRT-PCR. Total RNA extraction was carried out as described above. First, 1 μg of total RNA was taken to synthesize cDNA by using a PrimeScript II 1st-Strand cDNA synthesis kit (TaKaRa). The cDNA mixture was diluted to about 100 ng/μL and then used as the template for analyzing the gene expression level by quantitative reverse transcription-PCR (qRT-PCR) with SYBR Premix Ex Taq (TaKaRa, Japan) using an iQ5 continuous fluorescence detector system (Bio-Rad, Hercules, CA). Data were normalized to the β-actin gene *ACT1*. The primer sequences used for the qRT-PCR are listed in Table 3.

Yeast two-hybrid assays. All Y2H plasmids were based on either pGBKT7 (Gal4BD) as the DNA-binding domain (BD) plasmid or pGADT7 (Gal4AD) as the transcription-activating domain (AD) plasmid. The Gal4AD and Gal4BD plasmids (pGBKT7-*MED15*, pGBKT7-*MED15*$^{V76R/R84K}$, pGADT7-*HAP5*, pGADT7-*MGA2*, and pGADT7-*AFT1*) were cotransformed into the yeast *AH109* reporter strain. Positive clones were selected, grown in YNB medium, and then spotted onto synthetic dextrose (SD)-Leu-Trp plates and SD-Leu-Trp-His selective plates with the histidine biosynthesis inhibitor 1,2,4-aminotrizole (3-AT) at 30°C for 3 to 5 days.

Sterol and phospholipid measurement. Log-phase cells were incubated in YNB medium with or without 0.3% (vol/vol) acetic acid (4 mM H_2O_2 or 1.2 M NaCl) for 8 h and then collected and washed with

TABLE 2 Plasmids used in this study

Plasmid	Genotype	Source
pY26	2μm, Amp^r, *URA3*, P_{GPD}, P_{TEF}	Our laboratory
pY13	CENARS, Amp^r, *HIS3*, P_{MED15}	Our laboratory
YEplac181	2μm, Amp^r, *LEU2*	Our laboratory
pML104	2μm, Amp^r, *URA3*, P$_{SNR52}$-empty sgRNA cassette, P$_{TDH3}$-CAS9	Our laboratory
pGBKT7	Kan^r, *TRP1*, GAL4 DNA-binding domain fusion	Our laboratory
pGADT7	Amp^r, *LEU2*, GAL4 transcription-activating domain fusion	Our laboratory

TABLE 3 Primers used in this study

Function and primer	Sequence (5′–3′)
Deletion	
KIX-L-F1	CTAACAAGCAATTACATATTCCC
KIX-L-F2	GTATGGAAACTTCAAATGTTCAAGCAGTAACGGCGTTTTTC
KIX-R-F1	AAAACGCCGTTACTGCTTGAACATTTGAAGTTTCCATACTTT
KIX-R-F2	ATCCTTGGAAGGTGGATAGTG
ARV1-L-F1	CTTCGTCCTACAGTTTGCATAT
ARV1-L-F2	TCTGGGCCTCCATGTCGCTGCGTTTATCACAGCTAATATCTACTTT
ARV1/KanMX4-F1	GATATTAGCTGTGATAAACGCAGCGACATGGAGGCC
ARV1/KanMX4-F2	CTGGATATTTTTTTATTTGCTCGACACTGGATGGCGG
ARV1-R-F1	ACGCCGCCATCCAGTGTCGAGCAAATAAAAAAATATCCAGTATTAC
ARV1-R-F2	ACTTCAGGGCTGGCGTAC
GIT1-L-F1	GTAGTAATAGCGGCGTAGAATG
GIT1-L-F2	TCTGGGCCTCCATGTCGCTGTTTTTATCCTATTCTATTTTTTTGAT
GIT1/KanMX4-F1	AAAATAGAATAGGATAAAAACAGCGACATGGAGGCC
GIT1/KanMX4-F2	GGAAGAAATCGATACCAATTTCGACACTGGATGGCGG
GIT1-R-F1	ACGCCGCCATCCAGTGTCGAAATTGGTATCGATTTCTTCCTC
GIT1-R-F2	TCCAAAGCACTTATTTCTAGGTTA
PRY1-L-F1	ACGCACAGAGTCATTTCCC
PRY1-L-F2	TCTGGGCCTCCATGTCGCTGGATTTATCAATTACGGGATATTAAA
PRY1/KanMX4-F1	TATCCCGTAATTGATAAATCCAGCGACATGGAGGCC
PRY1/KanMX4-F2	ATGAAAACTTTTCTTGAAAGTCGACACTGGATGGCGG
PRY1-R-F1	ACGCCGCCATCCAGTGTCGACTTTCAAGAAAAGTTTTCATTGAT
PRY1-R-F2	AAGGAAGTTCTGTACGAAATGTAA
MCD4-L-F1	TAGTGTAACGGCTATCACATCAC
MCD4-L-F2	TCTGGGCCTCCATGTCGCTGTTTTTACAGATTTCAGTTGTATGAGT
MCD4/KanMX4-F1	ACAACTGAAATCTGTAAAAACAGCGACATGGAGGCC
MCD4/KanMX4-F2	ATAGCGGTGGGTATGTGAATTCGACACTGGATGGCGG
MCD4-R-F1	ACGCCGCCATCCAGTGTCGAATTCACATACCCACCGCTAT
MCD4-R-F2	AATGCCTCTTTTGTTTGTTAGTT
NFT1-L-F1	GGTCACGGAACATCACTTTC
NFT1-L-F2	TCTGGGCCTCCATGTCGCTGTCCTAAAAATTAATACTGTGAATCG
NFT1/KanMX4-F1	CACAGTATTAATTTTTAGGACAGCGACATGGAGGCC
NFT1/KanMX4-F2	CCCGCTAGCCCCGCATCCAATCGACACTGGATGGCGG
NFT1-R-F1	ACGCCGCCATCCAGTGTCGATTGGATGCGGGGCTAG
NFT1-R-F2	CCTGTGGGATGCAGCTTAT
CST6-L-F1	CTATTGGCGAAAATTAAGATAAG
CST6-L-F2	TCTGGGCCTCCATGTCGCTGTATCCTACCAAAAAGGTGTGG
CST6/KanMX4-F1	CACACCTTTTTGGTAGGATACAGCGACATGGAGGCC
CST6/KanMX4-F2	TTGTGCTCACCAAAACTTTGTCGACACTGGATGGCGG
CST6-R-F1	ACGCCGCCATCCAGTGTCGACAAAGTTTTGGTGAGCACAA
CST6-R-F2	CTGCTAAGGAAGCGATGGGACAC
HAP5-L-F1	TATGCAGTATTAAGATCCGTTTT
HAP5-L-F2	TCTGGGCCTCCATGTCGCTGTATGCGAGTAAACAATCCTGAT
HAP5/KanMX4-F1	CAGGATTGTTTACTCGCATACAGCGACATGGAGGCC
HAP5/KanMX4-F2	CTGTATAACCATTAACTCTCTCGACACTGGATGGCGG
HAP5-R-F1	ACGCCGCCATCCAGTGTCGAGAGAGTTAATGGTTATACAGCTGC
HAP5-R-F2	TTATGGCAGAAGATTGTGGTG
YAP1-L-F1	AAATAAGTACGGGAACGAGGTA
YAP1-L-F2	TCTGGGCCTCCATGTCGCTGGGTTTAAGAAACAACTTTTCCTTC
YAP1/KanMX4-F1	GAAAAGTTGTTTCTTAAACCCAGCGACATGGAGGCC
YAP1/KanMX4-F2	TTTTCCATAAAGTTCCCGCTTCGACACTGGATGGCGG
YAP1-R-F1	ACGCCGCCATCCAGTGTCGAAGCGGGAACTTTATGGAAA
YAP1-R-F2	GCCACTAACAAGGATAGAAAGC
AFT1-L-F1	ATTGACTGTTGGATGAAAGGGTA
AFT1-L-F2	TCTGGGCCTCCATGTCGCTGTGTCGTAGATTTTTCTGTTATTTTT
AFT1/KanMX4-F1	TAACAGAAAAATCTACGACACAGCGACATGGAGGCC
AFT1/KanMX4-F2	AGTTTGATTTCATCTATATGTCGACACTGGATGGCGG
AFT1-R-F1	ACGCCGCCATCCAGTGTCGACATATAGATGAAATCAAACTTAGACG
AFT1-R-F2	TCAATCACAACAAAGAAGAAAGG
STE12-L-F1	AACAACTCTTCGCGGTCAG
STE12-L-F2	TCTGGGCCTCCATGTCGCTGCCTTGGTGAACAAGACAATTC
STE12/KanMX4-F1	AATTGTCTTGTTCACCAAGGCAGCGACATGGAGGCC

(Continued on next page)

TABLE 3 (Continued)

Function and primer	Sequence (5′–3′)
STE12/KanMX4-F2	AATTCAAAAATTATATTATATCGACACTGGATGGCGG
STE12-R-F1	ACGCCGCCATCCAGTGTCGATATAATATAATTTTTGAATTTATGATACAAG
STE12-R-F2	CTAAGCGATCATGTAGTTTTGGA
MGA2-L-F1	AGAGCGATTGGATGACAGTTAC
MGA2-L-F2	TCTGGGCCTCCATGTCGCTGAACGAAATGTTCTGTTCGCC
MGA2/KanMX4-F1	GGCGAACAGAACATTTCGTTCAGCGACATGGAGGCC
MGA2/KanMX4-F2	TATATACGTAAAAAAGCAGATCGACACTGGATGGCGG
MGA2-R-F1	ACGCCGCCATCCAGTGTCGATCTGCTTTTTTACGTATATATATATATATATG
MGA2-R-F2	AGACACTACCAACCCTCACAAC
qRT-PCR	
ARV1-F1	ATCGCCTTTGGCTTCTACTA
ARV1-F2	TATTGGTGGGCTCCAGGTA
GIT1-F1	ATTTTAGATGGAAGACTGCTACTAC
GIT1-F2	GGTCCTTGATAACGGAACTG
NFT1-F1	CTAGTATGCCAATGGATAACAAA
NFT1-F2	GAAGACGGAACGAAGAGGTAA
ACT1-F1	CACTATTGGTAACGAAAGATTCAG
ACT1-F2	TAGAACCACCAATCCAGACG
Point mutation	
pY13/P_{MED15}-*MED15*-F1	ACTAAAGGGAACAAAAGCTGGAGCTCGGAGAACCGTGTTTGGAATT
pY13/P_{MED15}-*MED15*-F2	GTATCGATAAGCTTGATATCGAATTCTCAAGTAGCACTTGTCCAATTATT
pY13/P_{MED15}-*MED15* KIX-F2	GTATCGATAAGCTTGATATCGAATTCTCAAGCAGTAACGGCGTTTT
MED15^{N22A}-F1	GCGAAGAACGTCGCCGGGTTGCTTCAG
MED15^{N22A}-F2	GCGAAGAACGTCGCCGGGTTGCTTCAG
MED15^{L24A}-F1	AACGTCAACGGGGCGCTTCAGGTGCTC
MED15^{L24A}-F2	GAGCACCTGAAGCGCCCCGTTGACGTT
MED15^{L28A}-F1	TTGCTTCAGGTGGCCATGGACATTAAC
MED15^{L28A}-F2	GTTAATGTCCATGGCCACCTGAAGCAA
MED15^{I31A}-F1	GTGCTCATGGACGCTAACACTCTGAAC
MED15^{I31A}-F2	GTTCAGAGTGTTAGCGTCCATGAGCAC
MED15^{N32A}-F1	CTCATGGACATTGCCACTCTGAACGGA
MED15^{N32A}-F2	TCCGTTCAGAGTGGCAATGTCCATGAG
MED15^{N35A}-F1	ATTAACACTCTGGCCGGAGGGAGCTCC
MED15^{N35A}-F2	GGAGCTCCCTCCGGCCAGAGTGTTAAT
MED15^{K44A}-F1	GACACTGCTGATGCGATAAGAATTCAT
MED15^{K44A}-F2	ATGAATTCTTATCGCATCAGCAGTGTC
MED15^{I45A}-F1	ACTGCTGATAAGGCAAGAATTCATGCC
MED15^{I45A}-F2	GGCATGAATTCTTGCCTTATCAGCAGT
MED15^{H48A}-F1	AAGATAAGAATTGCTGCCAAAAACTTC
MED15^{H48A}-F2	GAAGTTTTTGGCAGCAATTCTTATCTT
MED15^{N51A}-F1	ATTCATGCCAAAGCCTTCGAGGCAGCT
MED15^{N51A}-F2	AGCTGCCTCGAAGGCTTTGGCATGAAT
MED15^{F52A}-F1	CATGCCAAAAACGCCGAGGCAGCTTTG
MED15^{F52A}-F2	CAAAGCTGCCTCGGCGTTTTTGGCATG
MED15^{L56A}-F1	TTCGAGGCAGCTGCGTTCGCAAAGAGC
MED15^{L56A}-F2	GCTCTTTGCGAACGCAGCTGCCTCGAA
MED15^{E65A}-F1	TCTTCAAAGAAAGCATACATGGACAGC
MED15^{E65A}-F2	GCTGTCCATGTATGCTTTCTTTGAAGA
MED15^{M67A}-F1	AAGAAAGCATACGCGGCCAGCATGAAC
MED15^{M67A}-F2	GTTCATGCTGGCCGCGTATGCTTTCTT
MED15^{S69A}-F1	GAATACATGGACGCCATGAACGAAAAA
MED15^{S69A}-F2	TTTTTCGTTCATGGCGTCCATGTATTC
MED15^{E72A}-F1	GACAGCATGAACGCAAAAGTTGCTGTC
MED15^{E72A}-F2	GACAGCAACTTTTGCGTTCATGCTGTC
MED15^{V76A}-F1	GAAAAAGTTGCTGCCATGCGCAACACG
MED15^{V76A}-F2	CGTGTTGCGCATGGCAGCAACTTTTTC
MED15^{M77A}-F1	AAAGTTGCTGTCGCGCGCAACACGTAC
MED15^{M77A}-F2	GTACGTGTTGCGCGCGACAGCAACTTT
MED15^{Y81A}-F1	ATGCGCAACACGGCCAATACGAGGAAA
MED15^{Y81A}-F2	TTTCCTCGTATTGGCCGTGTTGCGCAT
MED15^{R84A}-F1	ACGTACAATACGGCGAAAAACGCCGTT

(Continued on next page)

TABLE 3 (Continued)

Function and primer	Sequence (5′–3′)
MED15^{R84A}-F2	AACGGCGTTTTTCGCCGTATTGTACGT
MED15^{V76R}-F1	GAAAAAGTTGCTGCGATGCGCAACACG
MED15^{V76R}-F2	CGTGTTGCGCATCGCAGCAACTTTTTC
MED15^{R84R}-F1	ACGTACAATACGAAGAAAAACGCCGTT
MED15^{R84R}-F2	AACGGCGTTTTTCTTCGTATTGTACGT
eGFP expression	
ARV1/eGFP-F1	GCTATGACCATGATTACGCCAAGCTTCATACGATAATATGGTTTCTATACTGT
ARV1/eGFP-F2	TCCTCGCCCTTGCTCACCATTCTAGACGTTTATCACAGCTAATATCTACTTT
GIT1/eGFP-F1	GCTATGACCATGATTACGCCAAGCTTAAGATTCGAGTCTGGGTGC
GIT1/eGFP-F2	TCCTCGCCCTTGCTCACCATTCTAGATTTTTATCCTATTCTATTTTTTTGAT
NFT1/eGFP-F1	GCTATGACCATGATTACGCCAAGCTTAATTTCCTCCGTCCTACAAGTA
NFT1/eGFP-F2	TCCTCGCCCTTGCTCACCATTCTAGATCCTAAAAATTAATACTGTGAATCG
Yeast two-hybrid assay	
BD-*MED15*-F1	CGCCCGGGCCTCGAGCCCGGGTCGACATGTCTGCTGCTCCTGTCCAAG
BD-*MED15*-F2	TTCGCCCGGAATTAGCTTGGCTGCAGCTAAGTAGCACTTGTCCAATTATT
BD-*MED15*$^{V76R/R84K}$-F1	CGCCCGGGCCTCGAGCCCGGGTCGACATGTCTGCTGCTCCTGTCCAAG
BD-*MED15*$^{V76R/R84K}$-F2	TTCGCCCGGAATTAGCTTGGCTGCAGCTAAGTAGCACTTGTCCAATTATT
AD-*HAP5*-F1	TAGGATCCTCTGCTAGCAGAGAATTCATGACTGATAGGAATTTCTCACC
AD-*HAP5*-F2	CTCTAGAGTCGACTAATACTCTCGAGCTATTGTGGAAGAGGTCTTCTAG
AD-*MGA2*-F1	TAGGATCCTCTGCTAGCAGAGAATTCATGCAGCAGAACAGTGAGT
AD-*MGA2*-F2	CTCTAGAGTCGACTAATACTCTCGAGCTAACTGACAATTAAATCGTTCAACA
AD-*AFT1*-F1	TAGGATCCTCTGCTAGCAGAGAATTCATGGAAGGCTTCAATCCGG
AD-*AFT1*-F2	CTCTAGAGTCGACTAATACTCTCGAGCTAATCTTCTGGCTTCACATACT
Coimmunoprecipitation	
pY26/P$_{GPD}$-*MED15*-F1	GATTCTAGAACTAGTGGATCCATGTCTGCTGCTCCTGTCCAAG
pY26/P$_{GPD}$-*MED15*-F2	GTCGACGGTATCGATAAGCTTCTATACCCATACGACGTCCCAGACTACGCTAGTAGCACTTGTCCAATTATTCC
pY26/P$_{GPD}$-*MED15*$^{V76R/R84K}$-F1	GATTCTAGAACTAGTGGATCCATGTCTGCTGCTCCTGTCCAAG
pY26/P$_{GPD}$-*MED15*$^{V76R/R84K}$-F2	GTCGACGGTATCGATAAGCTTCTATACCCATACGACGTCCCAGACTACGCTAGTAGCACTTGTCCAATTATTCC
pY26/P$_{TEF}$-*HAP5*-F1	AAGTTTTCTAGAACTAGCGCGGCCGCATGACTGATAGGAATTTCTCACC
pY26/P$_{TEF}$-*HAP5*-F2	GGCGAAGAATTGTTAATTAAAGATCTCAGATCCTCTTCAGAGATGAGTTTCTGCTCTTGTGGAAGAGGTCTTCTAGGC
pY26/P$_{TEF}$-*MGA2*-F1	AAGTTTTCTAGAACTAGCGCGGCCGCATGCAGCAGAACAGTGAGT
pY26/P$_{TEF}$-*MGA2*-F2	GGCGAAGAATTGTTAATTAAAGATCTCAGATCCTCTTCAGAGATGAGTTTCTGCTCACTGACAATTAAATCGTTCAACATTC
pY26/P$_{TEF}$-*AFT1*-F1	AAGTTTTCTAGAACTAGCGCGGCCGCATGGAAGGCTTCAATCCGG
pY26/P$_{TEF}$-*AFT1*-F2	GGCGAAGAATTGTTAATTAAAGATCTCAGATCCTCTTCAGAGATGAGTTTCTGCTCATCTTCTGGCTTCACATACTTCA

PBS. Membrane sterols were extracted by a modified saponification method (13) and then analyzed by gas chromatography-mass spectrometry (69). The phospholipids were extracted as described previously (55) and then analyzed by electrospray ionization mass spectrometry (35).

Cell membrane integrity, fluidity, and permeability analysis. Log-phase cells were incubated in YNB medium with or without 0.3% (vol/vol) acetic acid (4 mM H_2O_2 or 1.2 M NaCl) for 8 h and then collected, washed, and resuspended with PBS. For membrane integrity and permeability analysis, samples were incubated with SYTOX (Sigma-Aldrich) at 30°C in dark for 5 min and then used for flow cytometry analysis (55). SYTOX green is a non-cell-membrane-permeable fluorescent dye that can only pass through the disordered area of the cell membrane and stain dead cells. The membrane integrity decreases when the proportion of the SYTOX-stained cells increases. Samples were also incubated with FM4-64 dye and SYTOX dye for laser scanning confocal microscopy analysis (LSCM). For membrane fluidity analysis, samples were incubated with 1 μL of 1 mmol/L 1,6-diphenyl-1,3,5-hexatriene (DPH; Sigma-Aldrich). The fluorescence intensity was measured by using a spectrofluorimeter (Photon Technology International, USA) with excitation at 360 nm and emission at 450 nm. The fluorescence anisotropy value (*r*) was calculated as described previously (2). Fluorescence anisotropy values and the membrane fluidity showed a negative correlation (13).

Measurement of intracellular Na^+ and K^+ concentrations. Log-phase cells were incubated in YNB medium with or without 1.2 M NaCl. First, 50-mL samples were collected every 2 h and then washed twice in ice-cold 10 mM $MgCl_2$, 10 mM $CaCl_2$, and 1 mM HEPES buffer. They were then resuspended in the same buffer. The intracellular Na^+ and K^+ contents were measured using a flame-graphite furnace atomic absorption spectrometer, as described previously (70).

Nft1 activity analysis. Log-phase cells expressing Nft1-Myc were grown in YNB medium with or without 1.2 M NaCl for 4 h and collected as described above. Vacuolar membranes were purified by Ficoll density gradient centrifugation, as described previously (71). The protein Nft1-HA were purified by incubation with anti-myc-conjugated magnetic beads (Bio-Rad) (72). The Nft1 activity was determined

according to the amount of inorganic phosphate (P_i) released from ATP at 750 nm in a reaction mixture, as described previously (13). The ATPase activity is expressed as micromoles of P_i released per minute per milligram of the total membrane protein.

Pyruvate production and analysis. The strains were cultivated at 30°C in flasks or bioreactor containing medium A containing (per L) the following: 80 g of glucose, 3 g of KH_2PO_4, 1.0 g of $MgSO_4 \cdot 7H_2O$, 3 g of sodium acetate, 18 μg of thiamine-HCl, 4.0 μg of biotin, 40 μg pyridoxine-HCl, and 0.8 μg of nicotinic acid with an initial OD_{600} biomass of 1.0. Fermentation was performed at 30°C. An HPLC system (Dionex UltiMate 3000 Series; Thermo Scientific, Waltham, MA) was used to determine the concentrations of glucose and organic acid. This involved an Aminex HPX-87H column (7.8 $\times$ 300 mm; Bio-Rad Laboratories, Inc., Hercules, CA) at 35°C with 0.05 mM sulfuric acid as the mobile phase. The injection volume was 10 μL, and the flow rate was 0.6 mL/min.

SUPPLEMENTAL MATERIAL

Supplemental material is available online only.

SUPPLEMENTAL FILE 1, PDF file, 0.7 MB.

SUPPLEMENTAL FILE 2, XLSX file, 0.04 MB.

ACKNOWLEDGMENTS

This study is supported by the National Key R&D Program of China (2019YFA0904900), the National Natural Science Foundation of China (21978113 and 32070124), the Key Program of the National Natural Science Foundation of China (22038005), and the National First-Class Discipline Program of Light Industry Technology and Engineering (LITE2018-08).

We acknowledge Jinqiu Zhou for the generous gift of *S. cerevisiae* with mediator subunit deletion Wei Song and Xin Xu for autodock and protein structure analysis.

Y.Q., C.G., X.C., and L.L. conceived the project and wrote the manuscript. Y.Q., Z.L., J.W., and X.M. designed and performed all the experiments. Y.Q., N.X., J.C., W.C., and L.L. analyzed the results.

We declare no conflict of interest.

REFERENCES

1. Caspeta L, Chen Y, Ghiaci P, Feizi A, Buskov S, Hallstrom B, Petranovic D, Nielsen J. 2014. Altered sterol composition renders yeast thermotolerant. Science 346:75–78. https://doi.org/10.1126/science.1258137.
2. Qi Y, Liu H, Yu J, Chen X, Liu L. 2017. Med15B regulates acid stress response and tolerance in *Candida glabrata* by altering membrane lipid composition. Appl Environ Microbiol 83:e01128-17. https://doi.org/10.1128/AEM.01128-17.
3. Olin-Sandoval V, Yu JSL, Miller-Fleming L, Alam MT, Kamrad S, Correia-Melo C, Haas R, Segal J, Navarro DAP, Herrera-Dominguez L, Mendez-Lucio O, Vowinckel J, Mulleder M, Ralser M. 2019. Lysine harvesting is an antioxidant strategy and triggers underground polyamine metabolism. Nature 572:249–253. https://doi.org/10.1038/s41586-019-1442-6.
4. Sévin DC, Sauer U. 2014. Ubiquinone accumulation improves osmotic-stress tolerance in *Escherichia coli*. Nat Chem Biol 10:266–272. https://doi.org/10.1038/nchembio.1437.
5. Sandoval N, Papoutsakis E. 2016. Engineering membrane and cell-wall programs for tolerance to toxic chemicals: beyond solo genes. Curr Opin Microbiol 33:56–66. https://doi.org/10.1016/j.mib.2016.06.005.
6. Kell D, Swainston N, Pir P, Oliver S. 2015. Membrane transporter engineering in industrial biotechnology and whole cell biocatalysis. Trends Biotechnol 33:237–246. https://doi.org/10.1016/j.tibtech.2015.02.001.
7. Li P, Fu X, Li S, Zhang L. 2018. Engineering TATA-binding protein Spt15 to improve ethanol tolerance and production in *Kluyveromyces marxianus*. Biotechnol Biofuels 11:207–219. https://doi.org/10.1186/s13068-018-1206-9.
8. Mitchell A, Wei P, Lim WA. 2015. Oscillatory stress stimulation uncovers an Achilles' heel of the yeast MAPK signaling network. Science 350:1379–1383. https://doi.org/10.1126/science.aab0892.
9. Tan F, Wu B, Dai L, Qin H, Shui Z, Wang J, Zhu Q, Hu G, He M. 2016. Using global transcription machinery engineering (gTME) to improve ethanol tolerance of *Zymomonas mobilis*. Microb Cell Fact 15:4–13. https://doi.org/10.1186/s12934-015-0398-y.
10. Alper H, Moxley J, Nevoigt E, Fink GR, Stephanopoulos G. 2006. Engineering yeast transcription machinery for improved ethanol tolerance and production. Science 314:1565–1569. https://doi.org/10.1126/science.1131969.
11. Lin ZL, Zhang Y, Wang JQ. 2013. Engineering of transcriptional regulators enhances microbial stress tolerance. Biotechnol Adv 31:986–991. https://doi.org/10.1016/j.biotechadv.2013.02.010.
12. Zhang H, Chong H, Ching CB, Jiang R. 2012. Random mutagenesis of global transcription factor cAMP receptor protein for improved osmotolerance. Biotechnol Bioeng 109:1165–1172. https://doi.org/10.1002/bit.24411.
13. Yan D, Lin X, Qi Y, Liu H, Chen X, Liu L, Chen J. 2016. Crz1p regulates pH homeostasis in *Candida glabrata* by altering membrane lipid composition. Appl Environ Microbiol 82:6920–6929. https://doi.org/10.1128/AEM.02186-16.
14. Tanaka K, Ishii Y, Ogawa J, Shima J. 2012. Enhancement of acetic acid tolerance in *Saccharomyces cerevisiae* by overexpression of the *HAA1* gene, encoding a transcriptional activator. Appl Environ Microbiol 78:8161–8163. https://doi.org/10.1128/AEM.02356-12.
15. Khalil AS, Lu TK, Bashor CJ, Ramirez CL, Pyenson NC, Joung JK, Collins JJ. 2012. A synthetic biology framework for programming eukaryotic transcription functions. Cell 150:647–658. https://doi.org/10.1016/j.cell.2012.05.045.
16. Ma C, Wei XW, Sun CH, Zhang F, Xu JR, Zhao XQ, Bai FW. 2015. Improvement of acetic acid tolerance of *Saccharomyces cerevisiae* using a zinc-finger-based artificial transcription factor and identification of novel genes involved in acetic acid tolerance. Appl Microbiol Biotechnol 99:2441–2449. https://doi.org/10.1007/s00253-014-6343-x.
17. Chen T, Wang J, Zeng L, Li R, Li J, Chen Y, Lin Z, Isalan M. 2012. Significant rewiring of the transcriptome and proteome of an *Escherichia coli* strain harboring a tailored exogenous global regulator IrrE. PLoS One 7:e37126. https://doi.org/10.1371/journal.pone.0037126.
18. Chen TJ, Wang JQ, Yang R, Li JC, Lin M, Lin ZL. 2011. Laboratory-evolved mutants of an exogenous global regulator, IrrE from *Deinococcus radiodurans*, enhance stress tolerances of *Escherichia coli*. PLoS One 6:e16228. https://doi.org/10.1371/journal.pone.0016228.
19. Yang YK, Zheng YT, Wang PC, Li X, Zhan CJ, Linhardt RJ, Zhang FM, Liu XX, Zhan JL, Bai ZH. 2020. Characterization and application of a putative transcription factor (*SUT2*) in *Pichia pastoris*. Mol Genet Genomics 295:1295–1304. https://doi.org/10.1007/s00438-020-01697-3.

20. Huang Z, Guo HD, Liu L, Jin SH, Zhu PL, Zhang YP, Jiang CZ. 2020. Heterologous expression of dehydration-inducible *Mf*WRKY17 of *Myrothamnus flabellifolia* confers drought and salt tolerance in *Arabidopsis*. Int J Mol Sci 21:4603. https://doi.org/10.3390/ijms21134603.
21. Song B, Zhou Q, Xue H-J, Liu J-J, Zheng Y-Y, Shen Y-B, Wang M, Luo J-M. 2018. IrrE Improves organic solvent tolerance and Δ^1-dehydrogenation productivity of *Arthrobacter simplex*. J Agric Food Chem 66:5210–5220. https://doi.org/10.1021/acs.jafc.8b01311.
22. Jeronimo C, Langelier MF, Bataille AR, Pascal JM, Pugh BF, Robert F. 2016. Tail and kinase modules differently regulate core Mediator recruitment and function *in vivo*. Mol Cell 64:455–466. https://doi.org/10.1016/j.molcel.2016.09.002.
23. Allen BL, Taatjes DJ. 2015. The Mediator complex: a central integrator of transcription. Nat Rev Mol Cell Biol 16:155–166. https://doi.org/10.1038/nrm3951.
24. Bourbon HM, Aguilera A, Ansari AZ, Asturias FJ, Berk AJ, Bjorklund S, Blackwell TK, Borggrefe T, Carey M, Carlson M, Conaway JW, Conaway RC, Emmons SW, Fondell JD, Freedman LP, Fukasawa T, Gustafsson CM, Han M, He X, Herman PK, Hinnebusch AG, Holmberg S, Holstege FC, Jaehning JA, Kim YJ, Kuras L, Leutz A, Lis JT, Meisterernest M, Naar AM, Nasmyth K, Parvin JD, Ptashne M, Reinberg D, Ronne H, Sadowski I, Sakurai H, Sipiczki M, Sternberg PW, Stillman DJ, Strich R, Struhl K, Svejstrup JQ, Tuck S, Winston F, Roeder RG, Kornberg RD. 2004. A unified nomenclature for protein subunits of Mediator complexes linking transcriptional regulators to RNA polymerase II. Mol Cell 14:553–557. https://doi.org/10.1016/j.molcel.2004.05.011.
25. Zhu XF, Chen LH, Carlsten JOP, Liu Q, Yang JS, Liu BD, Gustafsson CM. 2015. Mediator tail subunits can form amyloid-like aggregates *in vivo* and affect stress response in yeast. Nucleic Acids Res 43:7306–7314. https://doi.org/10.1093/nar/gkv629.
26. Nishikawa JL, Boeszoermenyi A, Vale-Silva LA, Torelli R, Posteraro B, Sohn Y-J, Ji F, Gelev V, Sanglard D, Sanguinetti M, Sadreyev RI, Mukherjee G, Bhyravabhotla J, Buhrlage SJ, Gray NS, Wagner G, Näär AM, Arthanari H. 2016. Inhibiting fungal multidrug resistance by disrupting an activator–Mediator interaction. Nature 530:485–489. https://doi.org/10.1038/nature16963.
27. Nogi Y, Fukasawa T. 1980. A novel mutation that affects utilization of galactose in *Saccharomyces cerevisiae*. Curr Genet 2:115–120. https://doi.org/10.1007/BF00420623.
28. Myers LC, Kornberg RD. 2000. Mediator of transcriptional regulation. Annu Rev Biochem 69:729–749. https://doi.org/10.1146/annurev.biochem.69.1.729.
29. Tuttle LM, Pacheco D, Warfield L, Luo J, Ranish J, Hahn S, Klevit RE. 2018. Gcn4-Mediator specificity is mediated by a large and dynamic fuzzy protein-protein complex. Cell Rep 22:3251–3264. https://doi.org/10.1016/j.celrep.2018.02.097.
30. Thakur JK, Arthanari H, Yang FJ, Pan SJ, Fan XC, Breger J, Frueh DP, Gulshan K, Li DK, Mylonakis E, Struhl K, Moye-Rowley WS, Cormack BP, Wagner G, Naar AM. 2008. A nuclear receptor-like pathway regulating multidrug resistance in fungi. Nature 452:604–612. https://doi.org/10.1038/nature06836.
31. Thakur JK, Arthanari H, Yang FJ, Chau KH, Wagner G, Naar AM. 2009. Mediator subunit Gal11p/MED15 is required for fatty acid-dependent gene activation by yeast transcription factor Oaf1p. J Biol Chem 284:4422–4428. https://doi.org/10.1074/jbc.M808263200.
32. Lin X, Qi Y, Yan D, Liu H, Chen X, Liu L. 2017. *CgMED3* changes membrane sterol composition to help *Candida glabrata* tolerate low pH stress. Appl Environ Microbiol 83:e00972-17. https://doi.org/10.1128/AEM.00972-17.
33. Kumar V, Waseem M, Dwivedi N, Maji S, Kumar A, Thakur JK. 2018. KIX domain of *At*Med15a, a Mediator subunit of *Arabidopsis*, is required for its interaction with different proteins. Plant Signal Behav 13:e1428514. https://doi.org/10.1080/15592324.2018.1428514.
34. Brzovic PS, Heikaus CC, Kisselev L, Vernon R, Herbig E, Pacheco D, Warfield L, Littlefield P, Baker D, Klevit RE, Hahn S. 2011. The acidic transcription activator Gcn4 binds the mediator subunit Gal11/Med15 using a simple protein interface forming a fuzzy complex. Mol Cell 44:942–953. https://doi.org/10.1016/j.molcel.2011.11.008.
35. Wu C, Zhang J, Zhu G, Yao R, Liu L. 2019. *Cg*Hog1-mediated *Cg*Rds2 phosphorylation alters glycerophospholipid composition to coordinate osmotic stress in *Candida glabrata*. Appl Environ Microbiol 85:e02822-18. https://doi.org/10.1128/AEM.02822-18.
36. Wu J, Chen XL, Cai LJ, Tang L, Liu LM. 2015. Transcription factors Asg1p and Hal9p regulate pH homeostasis in *Candida glabrata*. Front Microbiol 6:843–855.
37. McCourt P, Liu HY, Parker JE, Gallo-Ebert C, Donigan M, Bata A, Giordano C, Kelly SL, Nickels JT. 2016. Proper sterol distribution is required for *Candida albicans* hyphal formation and virulence. G3 (Bethesda) 6:3455–3465. https://doi.org/10.1534/g3.116.033969.
38. Holthuis J, Menon A. 2014. Lipid landscapes and pipelines in membrane homeostasis. Nature 510:48–57. https://doi.org/10.1038/nature13474.
39. Almaguer C, Fisher E, Patton-Vogt J. 2006. Posttranscriptional regulation of Git1p, the glycerophosphoinositol/glycerophosphocholine transporter of *Saccharomyces cerevisiae*. Curr Genet 50:367–375. https://doi.org/10.1007/s00294-006-0096-8.
40. Tan Z, Khakbaz P, Chen Y, Lombardo J, Yoon J, Shanks J, Klauda J, Jarboe L. 2017. Engineering *Escherichia coli* membrane phospholipid head distribution improves tolerance and production of biorenewables. Metab Eng 44:1–12. https://doi.org/10.1016/j.ymben.2017.08.006.
41. Singh-Babak SD, Shekhar T, Smith AM, Giaever G, Nislow C, Cowen LE. 2012. A novel calcineurin-independent activity of cyclosporin A in *Saccharomyces cerevisiae*. Mol Biosyst 8:2575–2584. https://doi.org/10.1039/c2mb25107h.
42. Gong Z, Nielsen J, Zhou YJ. 2017. Engineering robustness of microbial cell factories. Biotechnol J 12:1700014. https://doi.org/10.1002/biot.201700014.
43. Yin N, Zhu G, Luo Q, Liu J, Chen X, Liu L. 2020. Engineering of membrane phospholipid component enhances salt stress tolerance in *Saccharomyces cerevisiae*. Biotechnol Bioeng 117:710–720. https://doi.org/10.1002/bit.27244.
44. Fletcher E, Feizi A, Bisschops M, Hallstrom B, Khoomrung S, Siewers V, Nielsen J. 2017. Evolutionary engineering reveals divergent paths when yeast is adapted to different acidic environments. Metab Eng 39:19–28. https://doi.org/10.1016/j.ymben.2016.10.010.
45. Gao X, Yang X, Li J, Zhang Y, Chen P, Lin Z. 2018. Engineered global regulator H-NS improves the acid tolerance of *Escherichia coli*. Microb Cell Fact 17:118. https://doi.org/10.1186/s12934-018-0966-z.
46. Huang L, Pu Y, Yang XL, Zhu XC, Cai J, Xu ZN. 2015. Engineering of global regulator cAMP receptor protein (CRP) in *Escherichia coli* for improved lycopene production. J Biotechnol 199:55–61. https://doi.org/10.1016/j.jbiotec.2015.02.006.
47. Liu GD, Bergenholm D, Nielsen J. 2016. Genome-wide mapping of binding sites reveals multiple biological functions of the transcription factor Cst6p in *Saccharomyces cerevisiae*. mBio 7:e00559-16. https://doi.org/10.1128/mBio.00559-16.
48. Ortiz-Merino RA, Kuanyshev N, Byrne KP, Varela JA, Morrissey JP, Porro D, Wolfe KH, Branduardi P. 2018. Transcriptional response to lactic acid stress in the hybrid yeast *Zygosaccharomyces parabailii*. Appl Environ Microbiol 84:e02294-17. https://doi.org/10.1128/AEM.02294-17.
49. Swinnen S, Henriques SF, Shrestha R, Ho PW, Sa-Correia I, Nevoigt E. 2017. Improvement of yeast tolerance to acetic acid through Haa1 transcription factor engineering: towards the underlying mechanisms. Microb Cell Fact 16:7. https://doi.org/10.1186/s12934-016-0621-5.
50. Palma M, Guerreiro JF, Sa-Correia I. 2018. Adaptive response and tolerance to acetic acid in *Saccharomyces cerevisiae* and *Zygosaccharomyces bailii*: a physiological genomics perspective. Front Microbiol 9:274. https://doi.org/10.3389/fmicb.2018.00274.
51. Rossi A, Kontarakis Z, Gerri C, Nolte H, Hölper S, Krüger M, Stainier DYR. 2015. Genetic compensation induced by deleterious mutations but not gene knockdowns. Nature 524:230–233. https://doi.org/10.1038/nature14580.
52. Ma Z, Zhu P, Shi H, Guo L, Zhang Q, Chen Y, Chen S, Zhang Z, Peng J, Chen J. 2019. PTC-bearing mRNA elicits a genetic compensation response via Upf3a and COMPASS components. Nature 568:259–255. https://doi.org/10.1038/s41586-019-1057-y.
53. El-Brolosy MA, Kontarakis Z, Rossi A, Kuenne C, Günther S, Fukuda N, Kikhi K, Boezio GLM, Takacs CM, Lai S-L, Fukuda R, Gerri C, Giraldez AJ, Stainier DYR. 2019. Genetic compensation triggered by mutant mRNA degradation. Nature 568:193–195. https://doi.org/10.1038/s41586-019-1064-z.
54. Legras JL, Erny C, Le Jeune C, Lollier M, Adolphe Y, Demuyter C, Delobel P, Blondin B, Karst F. 2010. Activation of two different resistance mechanisms in *Saccharomyces cerevisiae* upon exposure to octanoic and decanoic aci. Appl Environ Microbiol 76:7526–7535. https://doi.org/10.1128/AEM.01280-10.
55. Qi YL, Liu H, Chen XL, Liu LM. 2019. Engineering microbial membranes to increase stress tolerance of industrial strains. Metab Eng 53:24–34. https://doi.org/10.1016/j.ymben.2018.12.010.
56. Degreif D, de Rond T, Bertl A, Keasling J, Budin I. 2017. Lipid engineering reveals regulatory roles for membrane fluidity in yeast flocculation and oxygen-limited growth. Metab Eng 41:46–56. https://doi.org/10.1016/j.ymben.2017.03.002.
57. Ballweg S, Ernst R. 2017. Control of membrane fluidity: the OLE pathway in focus. Biol Chem 398:215–228. https://doi.org/10.1515/hsz-2016-0277.

58. Tan Z, Yoon J, Nielsen D, Shanks J, Jarboe L. 2016. Membrane engineering via trans unsaturated fatty acids production improves *Escherichia coli* robustness and production of biorenewables. Metab Eng 35:105–113. https://doi.org/10.1016/j.ymben.2016.02.004.
59. Aguilera F, Peinado RA, Millán C, Ortega JM, Mauricio JC. 2006. Relationship between ethanol tolerance, H^+-ATPase activity and the lipid composition of the plasma membrane in different wine yeast strains. Int J Food Microbiol 110:34–42. https://doi.org/10.1016/j.ijfoodmicro.2006.02.002.
60. Zhu G, Yin N, Luo Q, Liu J, Wu J. 2020. Enhancement of sphingolipid synthesis improves osmotic tolerance of *Saccharomyces cerevisiae*. Appl Environ Microbiol 86:e02911-19.
61. Kamthan A, Kamthan M, Datta A. 2017. Expression of C-5 sterol desaturase from an edible mushroom in fission yeast enhances its ethanol and thermotolerance. PLoS One 12:e0173381. https://doi.org/10.1371/journal.pone.0173381.
62. Tan Z, Black W, Yoon JM, Shanks JV, Jarboe LR. 2017. Improving *Escherichia coli* membrane integrity and fatty acid production by expression tuning of FadL and OmpF. Microb Cell Fact 16:38–52. https://doi.org/10.1186/s12934-017-0650-8.
63. Walker C, Ryu S, Trinh CT. 2019. Exceptional solvent tolerance in *Yarrowia lipolytica* is enhanced by sterols. Metab Eng 54:83–95. https://doi.org/10.1016/j.ymben.2019.03.003.
64. Branco J, Ola M, Silva RM, Fonseca E, Gomes NC, Martins-Cruz C, Silva AP, Silva-Dias A, Pina-Vaz C, Erraught C, Brennan L, Rodrigues AG, Butler G, Miranda IM. 2017. Impact of *ERG3* mutations and expression of ergosterol genes controlled by *UPC2* and *NDT80* in *Candida parapsilosis* azole resistance. Clin Microbiol Infect 23:575–582.
65. Zhang M, Zhang K, Mehmood M, Zhao Z, Bai F, Zhao X. 2017. Deletion of acetate transporter gene *ADY2* improved tolerance of *Saccharomyces cerevisiae* against multiple stresses and enhanced ethanol production in the presence of acetic acid. Bioresour Technol 245:1461–1468. https://doi.org/10.1016/j.biortech.2017.05.191.
66. Guo Z, Khoomrung S, Nielsen J, Olsson L. 2018. Changes in lipid metabolism convey acid tolerance in *Saccharomyces cerevisiae*. Biotechnol Biofuels 11:297–311. https://doi.org/10.1186/s13068-018-1295-5.
67. Laughery MF, Hunter T, Brown A, Hoopes J, Ostbye T, Shumaker T, Wyrick JJ. 2015. New vectors for simple and streamlined CRISPR-Cas9 genome editing in *Saccharomyces cerevisiae*. Yeast 32:711–720. https://doi.org/10.1002/yea.3098.
68. Qu ZZ, Zhang LL, Zhu SM, Yuan W, Hang JW, Yin D, Tang XC, Zheng JY, Wang Z, Sun J. 2020. Overexpression of the transcription factor *HAC1* improves nerolidol production in engineered yeast. Enzyme Microb Technol 134:109485. https://doi.org/10.1016/j.enzmictec.2019.109485.
69. Tian HC, Zhou J, Qiao B, Liu Y, Xia JM, Yuan YJ. 2010. Lipidome profiling of *Saccharomyces cerevisiae* reveals pitching rate-dependent fermentative performance. Appl Microbiol Biotechnol 87:1507–1516. https://doi.org/10.1007/s00253-010-2615-2.
70. Li H, Liu W, Yang QS, Lin J, Chang YH. 2018. Isolation and comparative analysis of two Na^+/H^+ antiporter *NHX2* genes from *Pyrus betulaefolia*. Plant Mol Biol Rep 36:439–450. https://doi.org/10.1007/s11105-018-1089-8.
71. Owegi MA, Pappas DL, Finch MW, Bilbo SA, Resendiz CA, Jacquemin LJ, Warrier A, Trombley JD, McCulloch KM, Margalef KLM, Mertz MJ, Storms JM, Damin CA, Parra KJ. 2006. Identification of a domain in the Vo subunit d that is critical for coupling of the yeast vacuolar proton-translocating ATPase. J Biol Chem 281:30001–30014. https://doi.org/10.1074/jbc.M605006200.
72. Yao R, Shi L, Wu C, Qiao W, Liu L, Wu J. 2019. Lsm12 mediates deubiquitination of DNA polymerase η to help *Saccharomyces cerevisiae* resist oxidative stress. Appl Environ Microbiol 85:e01988-18. https://doi.org/10.1128/AEM.01988-18.
73. Peng J, Zhou JQ. 2012. The tail-module of yeast Mediator complex is required for telomere heterochromatin maintenance. Nucleic Acids Res 40:581–593. https://doi.org/10.1093/nar/gkr757.